ACS EARTH AND SPACE CHEMISTRY

http://pubs.acs.org/journal/aesccq
Article

Methodologies for ^{176}Lu–^{176}Hf Analysis of Zircon Grains from the Moon and Beyond

Xi Chen, Nicolas Dauphas,* Zhe J. Zhang, Blair Schoene, Melanie Barboni, Ingo Leya, Junjun Zhang, Dawid Szymanowski, and Kevin D. McKeegan

Cite This: *ACS Earth Space Chem.* 2024, 8, 36–53

ABSTRACT: Zircons are found in extraterrestrial rocks from the Moon, Mars, and some differentiated meteorite parent-bodies. These zircons are rare, often of small size, and have been affected by neutron capture induced by cosmic ray exposure. The application of the ^{176}Lu–^{176}Hf decay system to zircons from planetary bodies such as the Moon can help establish the chronology of large-scale differentiation processes such as the crystallization of the lunar magma ocean. Here, we present methods to measure the isotopic composition of Hf of extraterrestrial zircons dated using ID-TIMS U–Pb after chemical abrasion. We introduce a 2-stage elution scheme to separate Hf from Zr while preserving the unused Zr fraction for future isotopic analysis. The effect of neutron capture is also re-examined using the latest thermal neutron capture cross sections and epithermal resonance integrals. Our tests show that the precision of Hf isotopic analyses is close to what is theoretically attainable. We have tested this method to a limited set of zircon grains from lunar rocks returned by the Apollo missions (lunar soil 14163, fragmental polymict breccia 72275, and clast-rich breccia 14321). The model ages align with previously reported values, but further work is needed to assess the chronology of lunar magma ocean crystallization as only a handful of small zircons (5 zircons from 3 samples) were analyzed, and the precision of the analyses can be improved by measuring more and larger lunar zircon grains.

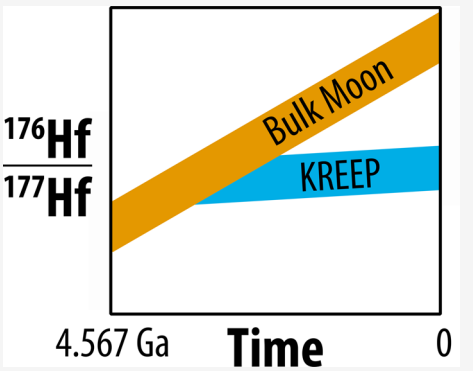

KEYWORDS: *zircon, dating, extraterrestrial, cosmogenic, differentiation*

INTRODUCTION

Zircon is a prime target mineral for ^{176}Lu–^{176}Hf studies (λ = 1.867× 10^{-11} yr^{-1}, $t_{1/2}$=37.12 Ga[1]) because it can readily be dated using U–Pb geochronology, has a low Lu/Hf ratio, and typically contains percent-level amounts of Hf. One can therefore measure present-day ^{176}Hf/^{177}Hf ratios in single zircon grains, either in bulk or through *in situ* techniques, and calculate the initial ^{176}Hf/^{177}Hf of the zircon with minimal correction for *in situ* decay of ^{176}Lu. Initial ^{176}Hf/^{177}Hf ratios can in turn be used to establish the history of planetary differentiation.[2−10] Zircons are relatively abundant in terrestrial rocks, and they are also found in lunar rocks and in meteorites from Mars and Vesta. Studies of extraterrestrial zircons present specific challenges that are seldom encountered in terrestrial rocks, arising from the scarcity and scientific value of their host rocks and the need to correct for shifts in Hf isotopic abundances induced by exposure to cosmic rays in space. D'Abzac et al.[11] and Bauer et al.[12] developed protocols for measuring the isotopic composition of Hf in small zircon and baddeleyite grains. They did not purify Hf and opted instead to monitor and correct isobaric interference during analysis. Bast et al.[13] also focused on small samples, but they purified Hf before isotopic analysis using a two-stage ion-exchange chromatography for Lu–Hf dating. We also employ ion chromatography for Hf purification, but our method is tailored for extraterrestrial zircons, where factors such as cosmogenic effects and normalization to chondrites are of concern.

Lunar zircons likely formed by either (*i*) crystallization of the lunar magma ocean[14,15] from a liquid named KREEP that is highly enriched in incompatible elements such as K, REE, and P[16,17] or (*ii*) later impact-induced melting.[18,19] KREEP is found in dilute form in basalts and soils recovered from the Moon by the Apollo missions. The KREEP component is highly enriched in Zr relative to the bulk silicate Moon (by a factor of ∼165[17]), leading to zircon crystallization in KREEP-rich magmas. Combining U–Pb and ^{176}Lu–^{176}Hf analyses of lunar zircons, one can estimate the initial ^{176}Hf/^{177}Hf ratio at the time of crystallization of lunar zircons, which should represent a snapshot of the composition of the KREEP reservoir at that time. KREEP is an enriched reservoir characterized by a low Lu/Hf ratio and unradiogenic ^{176}Hf/^{177}Hf ratios relative to those of

Received: April 12, 2023
Revised: November 8, 2023
Accepted: November 8, 2023
Published: December 7, 2023

https://doi.org/10.1021/acsearthspacechem.3c00093
ACS Earth Space Chem. 2024, 8, 36–53

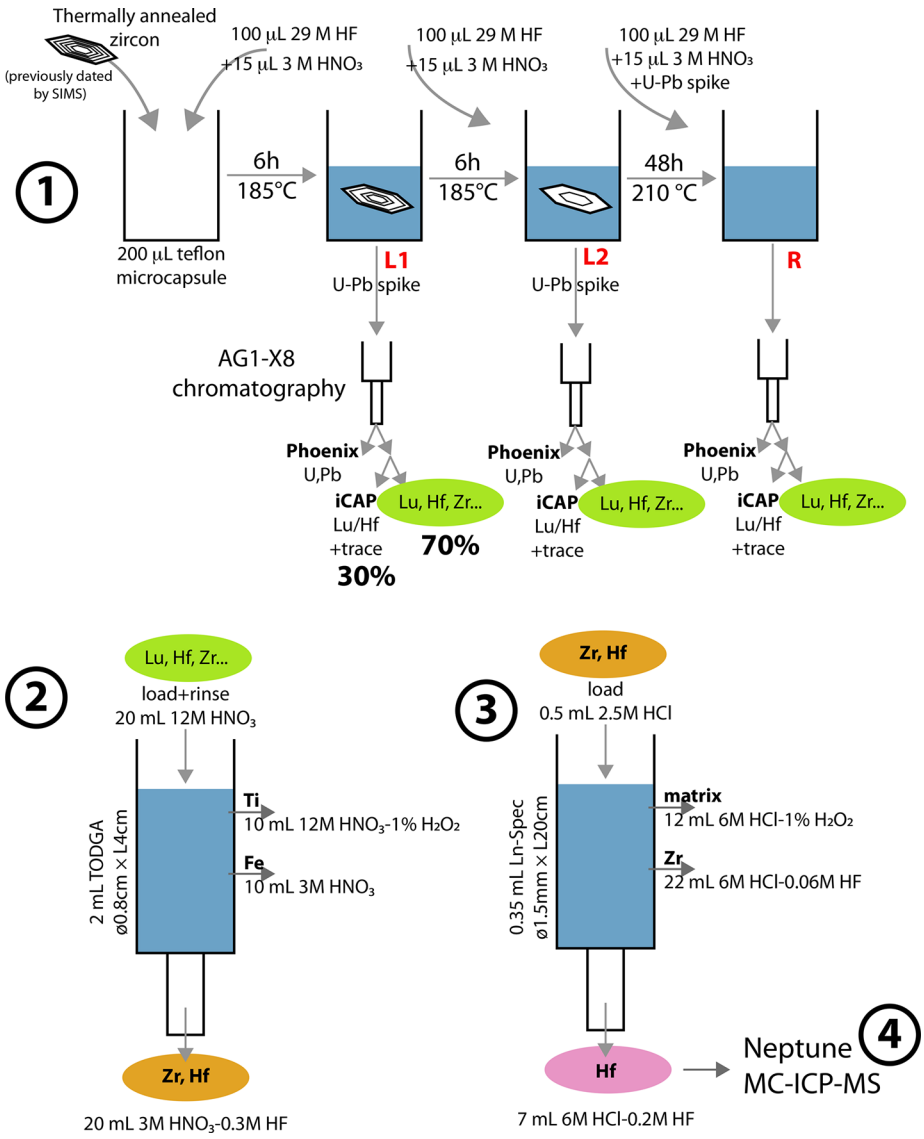

Figure 1. Flowchart of the procedure used for Lu−Hf analysis of extraterrestrial zircons. 1. The zircons are thermally annealed and then subjected to chemical abrasion.[2,69] Two leachates (L1 and L2) and one residue (R) solutions are retrieved for further processing. The solutions are passed on chromatography columns filled with AG1-X8 resin to separate U+Pb from a solution containing Lu, Hf, Zr, and other trace elements. The U+Pb elutions are analyzed using a Phoenix TIMS at Princeton University. The solution containing Lu, Hf, Zr, and other trace elements is split into two, with 30% used for Lu/Hf determination using an iCAP at Princeton University, and 70% used for Hf purification and Hf isotopic analysis at the Origins Lab of the University of Chicago. 2. The "Lu, Hf, Zr" 70% split solution is passed on a column filled with DGA resin[52,53] to separate Zr+Hf from most other elements. 3. The Zr+Hf cut is passed on a second column filled with Ln-Spec resin (Figure 2) to separate Hf from Zr.[27,50] 4. The isotopic composition of purified Hf is analyzed with a Neptune MC-ICP-MS at the University of Chicago.

the bulk silicate Moon (BSM) and the Chondritic Uniform Reservoir (CHUR). Comparison of the initial $^{176}Hf/^{177}Hf$ ratios of zircons with the inferred BSM value at the time of zircon crystallization can yield tight constraints on the time of LMO crystallization, which provides a minimum age for the formation of the Moon itself.[2,10]

Taylor et al.[10] analyzed the Hf isotopic compositions of lunar zircon grains from three polymict breccias and a soil collected by the Apollo 14 mission. The $^{176}Lu-^{176}Hf$ isotopic analyses were performed by laser-ablation multicollector inductively coupled plasma mass spectrometry (LA-MC-ICP-MS) on zircons that had been dated using U−Pb geochronology by secondary ionization mass spectrometry (SIMS). A virtue of *in situ* isotopic analyses is that the samples are not totally consumed during analysis and such analyses can resolve complex zircon growth histories, which can confound bulk zircon analyses.[7] The main limitations of *in situ* analyses are precision and accuracy since some isobaric interferences such as ^{176}Lu and ^{176}Yb on ^{176}Hf cannot be eliminated and must be corrected for. The data of Taylor et al.[10] favored termination of lunar magma ocean (LMO) crystallization ~ 70 Myr (~4500 Ma) after solar system formation but were permissive of an age as late as 120 Myr (~4450 Ma). To better define that age, Barboni et al.[2] measured $^{176}Hf/^{177}Hf$ ratios by MC-ICP-MS after zircon digestion, while U−Pb dates were obtained by isotope dilution thermal ionization mass spectrometry (ID-TIMS) on chemically abraded zircons. The samples that they analyzed were four zircon fragments from the same sample set that had been studied previously by Taylor et al.,[10] and an additional four affected by larger neutron capture effects. Barboni et al.[2] found very

https://doi.org/10.1021/acsearthspacechem.3c00093
ACS Earth Space Chem. 2024, 8, 36−53

Table 1. Chromatographic Purification Protocol for Zr and Hf

column 1 (2 mL DGA; 0.8 cm diameter × 4 cm length)			column 2 (0.35 mL Ln-Spec; 1.5 mm diameter × 20 cm length)		
step	volume (mL)	acid	step	volume (mL)	acid
clean	10	3 M HNO_3	clean	18	6 M HCl−0.06 M HF
	10	3 M HNO_3−1 vol% H_2O_2		14	6 M HCl−0.2 M HF
	4	H_2O	precondition	6	2.5 M HCl
precondition	15	12 M HNO_3	load	0.5	2.5 M HCl
load	10	12 M HNO_3	rinse matrix	12	6 M HCl−1 vol% H_2O_2
rinse matrix	10	12 M HNO_3	elute Zr	22	6 M HCl−0.06 M HF
Elute Ti	10	12 M HNO_3−1 vol% H_2O_2	Hf	7	6 M HCl−0.2 M HF
Fe	10	3 M HNO_3			
Zr and Hf	20	3 M HNO_3−0.3 M HF			

unradiogenic $^{176}Hf/^{177}Hf$ ratios in several zircons, suggesting early crystallization of the LMO. They concluded that LMO crystallization must have been completed within ∼60 Myr (>4507 Ma) of the formation of the solar system, but the precision of the Hf isotopic measurements was limited and only a handful of samples were analyzed. A model age of KREEP was also estimated using ^{147}Sm-^{143}Nd and ^{176}Lu−^{176}Hf isochron analyses of KREEP-rich rock samples (Borg and Carlson[20] and references therein). These two decay systems yielded rock-scale model ages of 4334 ± 37 Ma and 4356 ± 37 Ma for KREEP (∼220 Myr after solar system formation). There is thus considerable uncertainty on when LMO crystallization finished, with zircon and rock model ages giving values between ∼60 and ∼220 Myr after solar system formation.[2,10,21−23] Taylor et al.[10] and Barboni et al.[2] reported precisions on $^{176}Hf/^{177}Hf$ measurements of 1 to 4 ε-units at 2σ ($\varepsilon^{176}Hf$ is the deviation in parts per 10^4 of the $^{176}Hf/^{177}Hf$ ratio relative to a reference material) on grain fragments that were 60−150 μm in size originally, but part of those grains had been consumed by prior laser ablation work. Higher precision and accuracy measurements are needed to provide more robust constraints on the formation of KREEP, which represents a firm minimum limit on the age of the Moon itself.[2]

Combined $^{176}Hf/^{177}Hf$ and U−Pb measurements of zircons can also provide insights into the early differentiation history of Mars. Bouvier et al.[24] and Costa et al.[6] studied ancient zircons (4.43 to 4.48 Ga $^{207}Pb/^{206}Pb$ ages) extracted from martian polymict breccia NWA 7533/NWA 7034, also known as Black Beauty. The $^{176}Hf/^{177}Hf$ ratios measured in those zircons pointed to the existence of an enriched crustal reservoir on Mars that formed ∼20 Myr after solar system formation. The extracted Martian zircon grains were 30 to 80 μm in size, and the precision of $\varepsilon^{176}Hf$ isotopic analyses ranged from ∼±0.3 to ± 1.

Iizuka et al.[25] measured $^{176}Hf/^{177}Hf$ ratios in zircon grains extracted from the Agoult eucrite meteorite. Eucrites are basaltic meteorites that are thought to have formed in the crust of asteroid Vesta soon after the formation of the solar system. Iizuka et al.[25] used these measurements to constrain the solar system initial $^{176}Hf/^{177}Hf$ ratio (0.279781 ± 0.000018). The typical size of zircon grains in eucrites is ∼20 μm, but those extracted from Agoult were ∼80 μm. The precisions obtained on $\varepsilon^{176}Hf$ isotopic analyses in these zircons ranged from ∼±0.3 to ±1.

Extraterrestrial zircons are precious and data quality is paramount as a handful of measurements can have large scale implications on the chronology of planetary differentiation.[2,6,10,24,25] As a part of an effort to better understand the magmatic differentiation and early bombardment history of the Moon, we developed an analytical protocol to analyze Lu−Hf isotope systematics in small single zircon grains. Building on previous studies,[25−28] we developed a protocol to first isolate Zr and Hf from interfering Yb and Lu elements and then further purify Zr from Hf. Peters et al.[29] found that inefficient removal of Zr from the Hf cut leads to unusual mass bias behavior and matrix-dependent effects on measured Hf isotopic ratios when using Jet-sampler and X-skimmer cones. By removing Zr, we can therefore take advantage of the higher sensitivity of these cones without compromising the accuracy of Hf isotopic analyses. Another motivation for this second step is to allow future isotopic analyses of Zr on the same sample aliquots for the study of Zr mass-dependent isotopic fractionation,[30−39] nucleosynthetic anomalies,[40−45] and decay of extinct radionuclide ^{92}Nb into ^{92}Zr.[46−49] Hafnium isotopic analyses are done by MC-ICP-MS. We also compare achieved and theoretically attainable precision for internally normalized ratios based on counting statistics and Johnson noise.

METHODS

The method developed combines chemical abrasion of zircons, U−Pb dating by TIMS, Lu/Hf determination using a quadrupole ICP-MS, purification of Hf in a 2-stage chromatographic procedure using DGA and Ln-Spec resin, and Hf isotopic analysis by MC-ICP-MS. The various steps involved are outlined in Figure 1 and described in detail below.

Zirconium and Hafnium Separation. A two-stage procedure modified from Zhang[50] and Iizuka et al.[25] was developed for separating Zr and Hf from Yb, Lu and other interfering elements (Table 1; Figure 1). In a first step, DGA (*N*,*N*,*N*′,*N*′-tetra-n-octyldiglycolamide) resin from Eichrom (previously TODGA; now DGA normal[51,52]) is used to collect a Zr−Hf cut, as described by Zhang et al.[53] in their protocol for Ti separation. In a second step, Ln-Spec resin is used to further separate heavy rare earth elements (REEs), Zr and Hf (Table 1).[50]

The first step uses a 2-mL column of 0.8 cm diameter and 4 cm length, filled with DGA resin. The resin in the column is cleaned using 10 mL of 3 M HNO_3, 10 mL of 3 M HNO_3 + 1 vol % H_2O_2, and 4 mL of H_2O. The resin is conditioned using 15 mL of 12 M HNO_3. The sample is then loaded in 10 mL of 12 M HNO_3. Loading the sample in 12 M HNO_3 + 1 vol % H_2O_2 instead of 12 M HNO_3, as we have done, would expedite Ti elution and slightly reduce the blank. Titanium is eluted with 10 mL of 12 M HNO_3 + 1 vol % H_2O_2. Iron is eluted with 10 mL of 3 M HNO_3. Finally, Zr and Hf are eluted together with 20 mL of 3 M HNO_3−0.3 M HF. The Zr and Hf cut is dried down on a hot plate and taken up in 0.5 mL of 2.5 M HCl.

https://doi.org/10.1021/acsearthspacechem.3c00093
ACS Earth Space Chem. 2024, 8, 36−53

To optimize the chemical separation procedure in the second step, the elution curve was calibrated using a multielement standard solution containing Zr, Hf, and 24 other elements, including all the HFSEs and REEs (Figure 2). Single element

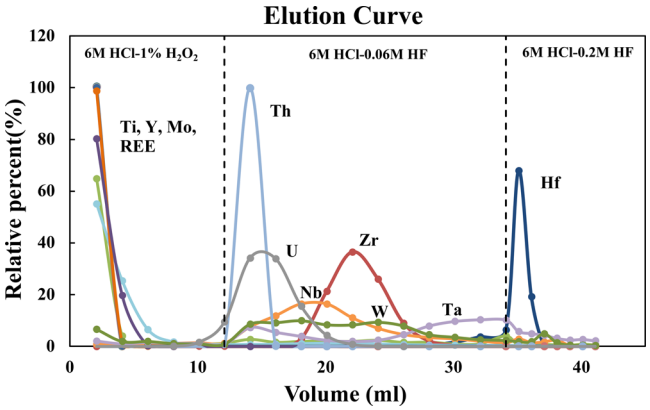

Figure 2. Elution curve of a multielement standard solution on a 0.35 mL Teflon column loaded with Ln-Spec resin. This corresponds approximately to the second step of our Hf purification procedure. Matrix elements were removed with 12 mL of 6 M HCL−1 vol% H_2O_2. Zirconium was first eluted in 22 mL of 6 M HCL−0.06 M HF. Hafnium was finally eluted in 7 mL of 6 M HCL−0.2 M HF. The elution sequence is from Zhang et al.[50]

ICP-MS standard solutions (Spex CertiPrep) at concentrations of 1000 μg/mL were used to prepare this standard mixture. A similar calibration was done using solutions retrieved after U−Pb chemistry of terrestrial zircon reference materials (AS3, 91500) and synthetic zircon doped with REEs (MUNZirc 32a[54]) (Figure 3). Zirconium and hafnium purifications of the standard mixture and the reference zircon solutions were done using a 0.35 mL fluoropolymer column (length = 20 cm, diameter = 1.5 mm) loaded with Ln-Spec resin (100−150 μm; HDEHP). Liquid was forced through the column using a pressure differential established by a vacuum box positioned below the column, with the vacuum pressure adjusted to

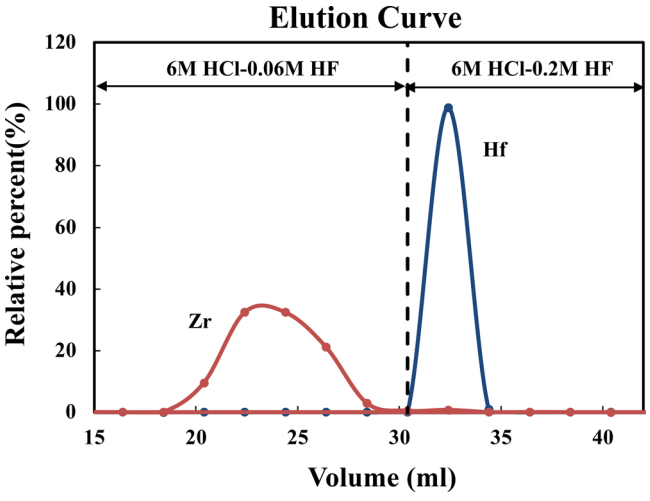

Figure 3. Elution curve of terrestrial zircon standard AS3 retrieved after U−Pb chemistry on a 0.35 mL Teflon column loaded with Ln-Spec resin. Matrix elements were removed with 12 mL of 6 M HCL−1 vol % H_2O_2. Zirconium was first eluted in 22 mL of 6 M HCL−0.06 M HF. Hafnium was finally eluted in 7 mL of 6 M HCl−0.2 M HF.

maintain a flow rate of ∼1−2 mL/hr. The resin was cleaned with 18 mL of 6 M HCl-0.06 M HF followed by 14 mL of 6 M HCl-0.2 M HF to ensure the removal of Zr and Hf that might be in the resin before loading the samples. The column filled with resin was preconditioned with 6 mL of 2.5 M HCl. The sample solutions were loaded onto the column in ∼0.5 mL of 2.5 M HCl and matrix elements were removed with 12 mL of 6 M HCl−1 vol % H_2O_2. Zirconium was first eluted in 22 mL of 6 M HCl−0.06 M HF. Hafnium was finally eluted in 7 mL of 6 M HCl−0.2 M HF (Table 1). Several studies have previously used the Ln-spec resin for separating Zr, Lu, and Hf. Münker et al.[27] developed an elution protocol that can handle various rock types. They loaded the samples in 3 M HCl + 0.1 M ascorbic acid, rinsed the matrix in 3 M HCl, eluted Lu in 6 M HCl, eluted Ti in 0.09 M citric acid−0.4 M HNO_3−1 vol % H_2O_2, eluted Zr in 6 M HCl−0.06 M HF, and eluted Hf in 6 M HCl−0.2 M HF. The acids used for eluting Zr and Hf are identical with ours. Iizuka et al.[25] used a simpler procedure for extraterrestrial zircons. They loaded their samples in 2.5 M HCl, removed the matrix in 6 M HCl + 0.06 M HF, eluted Zr in 6 M HCl + 0.06 M HF, and eluted Hf in 2 M HF. Our procedure uses 6 M HCl throughout, with other reagents added to target specific elements (1 vol% H_2O_2 for Ti, 0.06 M HF for Zr, 0.2 M HF for Hf), which simplifies reagent preparation.

Following chromatographic separation, the Zr and Hf cuts were dried down, taken back up in ∼1 mL of aqua regia (3:1 mixture of HCl:HNO_3), and dried again before being redissolved in concentrated HNO_3. The redissolved solutions were dried again to near dryness (right before complete evaporation) and taken back up in 0.3 M HNO_3−0.07 M HF for Hf isotopic analysis. The Hf procedural blank was below detection limit (<5 pg) and was negligible compared to the amount of Hf in the single zircon grains analyzed (>4000 pg).

Hafnium Isotope Mass Spectrometry. The Hf isotopic analyses were done on a Neptune MC-ICP-MS instrument upgraded with a Pfeiffer OnTool Booster turbo pump to Neptune Plus specifications. The samples in 0.3 M HNO_3−0.07 M HF were injected into the Ar plasma torch using an Aridus II desolvating nebulizer. The sample, auxiliary, and cooling gas flows were set to ∼0.825, 1, and 16 mL/min, respectively. The Ar and N_2 gas flows of the Aridus II nebulizer were set to 7.3 and 0.14 mL/min, respectively. High-transmission Jet sample and X-skimmer cones were used. All measurements were done in low resolution. The purified Hf fractions were dissolved in 0.3 M HNO_3-0.07 M HF. The sensitivity was ∼0.2 V/ppb on ^{177}Hf (18.60%) measured on a 10^{11} Ω amplifier at a sample uptake rate of ∼100 μL/min. Isotopes ^{174}Hf, ^{176}Hf, ^{177}Hf, ^{178}Hf, ^{179}Hf, and ^{180}Hf, as well as ^{172}Yb, ^{175}Lu, and ^{184}W were measured in static mode on 9 Faraday cups with ^{172}Yb and ^{174}Hf Faraday cups connected to 10^{12} Ω amplifiers and other cups connected to 10^{11} Ω amplifiers. Isotope ^{172}Yb was measured to monitor possible interferences from ^{174}Yb and ^{176}Yb. Isotope ^{175}Lu was measured to monitor a possible interference from ^{176}Lu. Isotope ^{184}W was measured to monitor a possible interference from ^{180}W. All potential isobaric interferences from Yb, Lu, and W on Hf isotopes were corrected for, but these were always negligible, which is expected given the low Yb/Hf, Lu/Hf, and W/Hf ratios of zircons and the high selectivity of the Hf-Zr purification procedure outlined above. Hafnium was diluted to ∼1−10 ppb for isotopic analysis. The measurements were divided into 30 cycles of 8.389 s integration time each. The 0.3 M HNO_3−0.07 M HF dilution medium was measured at the beginning and at the end of each sequence run, and average intensities were

https://doi.org/10.1021/acsearthspacechem.3c00093
ACS Earth Space Chem. 2024, 8, 36−53

subtracted from sample and standard measurements (on peak zero). Individual sample measurements were bracketed by the analysis of JMC-Hf 475 standard solutions whose concentrations were adjusted to match those of the samples that they bracket.

Natural processes[55] and mass spectrometry[56] induce Hf isotopic fractionation that must be corrected for before discussing ^{176}Hf variations arising from decay of ^{176}Lu. Mass bias (β) was calculated by normalizing ^{179}Hf/^{177}Hf ratios in the samples and bracketing standards to a fixed reference value of 0.7325[57] using the exponential mass fractionation law $r_{2/1} = R_{2/1}(m_2/m_1)^{\beta}$ with $r_{2/1}$ and $R_{2/1}$ the measured (meas) and "unfractionated" (ref) ratios, respectively, and m_2/m_1 the ratio of the atomic masses of the two isotopes,[58]

$$\beta = \ln\left[\left(\frac{^{179}\mathrm{Hf}}{^{177}\mathrm{Hf}}\right)_{\mathrm{meas}} \Big/ \left(\frac{^{179}\mathrm{Hf}}{^{177}\mathrm{Hf}}\right)_{\mathrm{ref}}\right] / \ln(m_{^{179}\mathrm{Hf}}/m_{^{177}\mathrm{Hf}}) \quad (1)$$

where m_i is the atomic mass of isotope i and ^{179}Hf/^{177}Hf$_{\mathrm{ref}}$ = 0.7325. The possible contributions of isobaric interferences on ^{176}Hf and ^{180}Hf were calculated assuming that Yb, Lu, and W would show approximately the same mass bias as Hf ($\beta_{\mathrm{Yb}} = \beta_{\mathrm{Lu}} = \beta_{\mathrm{W}} = \beta_{\mathrm{Hf}}$),

$$^{176}\mathrm{Hf} = I_{176} - I_{172}\left(\frac{^{176}\mathrm{Yb}}{^{172}\mathrm{Yb}}\right)_{\mathrm{ref}}\left(\frac{m_{^{176}\mathrm{Yb}}}{m_{^{172}\mathrm{Yb}}}\right)^{\beta} - I_{175}\left(\frac{^{176}\mathrm{Lu}}{^{175}\mathrm{Lu}}\right)_{\mathrm{ref}}\left(\frac{m_{^{176}\mathrm{Lu}}}{m_{^{175}\mathrm{Lu}}}\right)^{\beta} \quad (2)$$

$$^{180}\mathrm{Hf} = I_{180} - I_{184}\left(\frac{^{180}\mathrm{W}}{^{184}\mathrm{W}}\right)_{\mathrm{ref}}\left(\frac{m_{^{180}\mathrm{W}}}{m_{^{184}\mathrm{W}}}\right)^{\beta} \quad (3)$$

where I_k is the ion intensity measured at mass k after on-peak-zero subtraction and "ref" stands for reference and corresponds to the typical terrestrial isotopic composition for the elements considered: $(^{174}\mathrm{Yb}/^{172}\mathrm{Yb})_{\mathrm{ref}}$ = 1.458085, $(^{176}\mathrm{Yb}/^{172}\mathrm{Yb})_{\mathrm{ref}}$ = 0.584517, $(^{176}\mathrm{Lu}/^{175}\mathrm{Lu})_{\mathrm{ref}}$ = 0.026525, and $(^{180}\mathrm{W}/^{185}\mathrm{W})_{\mathrm{ref}}$ = 0.004086. These interference corrections were always negligible but were implemented to streamline the data reduction procedure in case an outlier sample requiring significant correction was analyzed. After on-peak-zero (baseline) subtraction and correction of isobaric interferences, ^{i}Hf/^{177}Hf ratios are corrected for mass fractionation based on the mass bias calculated from the ^{179}Hf/^{177}Hf ratio (the star superscript indicates that the ratio has been corrected for mass-fractionation by internal normalization),

$$\left(\frac{^{i}\mathrm{Hf}}{^{177}\mathrm{Hf}}\right)^{*} = \left(\frac{^{i}\mathrm{Hf}}{^{177}\mathrm{Hf}}\right)_{\mathrm{meas}} \Big/ \left(\frac{m_{^{i}\mathrm{Hf}}}{m_{^{177}\mathrm{Hf}}}\right)^{\beta} \quad (4)$$

The sample solutions were measured in a sequence standard-sample standard (STD1-SMP-STD2), with the bracketing standard being a solution of JMC-Hf 475 diluted to a sample-matched concentration in the same acid mixture as the sample. For each bracket j, ε^{i}Hf values are calculated as,

$$\varepsilon^{i}\mathrm{Hf}_{\mathrm{SMP},j} = \left[\frac{2(^{i}\mathrm{Hf}/^{177}\mathrm{Hf})^{*}_{\mathrm{SMP},j}}{(^{i}\mathrm{Hf}/^{177}\mathrm{Hf})^{*}_{\mathrm{STD1},j} + (^{i}\mathrm{Hf}/^{177}\mathrm{Hf})^{*}_{\mathrm{STD2},j}} - 1\right] \times 10^{4} \quad (5)$$

Depending on the zircon size and amount of Hf available, several bracket measurements were done (n = 1 to 4; each bracket analysis consumed ~5 ng of Hf). The reported Hf isotopic composition for a sample is the average of these n bracket measurements, $\varepsilon^{i}\mathrm{Hf}_{\mathrm{SMP}} = \sum_{j=1}^{n}\varepsilon^{i}\mathrm{Hf}_{\mathrm{SMP},j}/n$. For the purpose of comparing our data with previous studies, εHf values were also converted to absolute ratios using the following values for the isotopic ratios of the Johnson Matthey Company standard (JMC)-Hf 475: ^{180}Hf/^{177}Hf = 1.886666, ^{178}Hf/^{177}Hf = 1.467168, and ^{176}Hf/^{177}Hf = 0.282160.[59] We also calculated $\varepsilon^{i}\mathrm{Hf}_{\mathrm{STD},p}$ of the standard bracketed by itself, with $\varepsilon^{i}\mathrm{Hf}_{\mathrm{STD},p}$ defined as the ε^{i} Hf value of STD$_p$ bracketed by STD$_{p-1}$ and STD$_{p+1}$ in a sequence STD$_{p-1}$−SMP−STD$_p$−SMP−STD$_{p+1}$. These standards were measured at the same concentration in the same conditions as the sample, so we use the standard deviation of these standard bracket isotopic analyses $\sigma(\varepsilon^{i}\mathrm{Hf}_{\mathrm{STD}})$ to calculate the uncertainty of the mean sample isotopic composition, $\sigma(\varepsilon^{i})\mathrm{Hf}_{\mathrm{SMP}} = \sigma(\varepsilon^{i})\mathrm{Hf}_{\mathrm{STD}}$. The reason for doing so is that there were more repeats of standard bracketed by standards than sample bracketed by standards, so calculation of the standard deviation is more reliable. Another approach to calculating uncertainties would be to use the dispersion of repeat cycles within a single analysis. We find good agreement between the two approaches (Figure 4) but use repeat standard analyses to calculate error bars because it measures dispersion over a timespan that is more relevant to sample analyses (fluctuations happening in a matter of hours as opposed to minutes) and should be more reliable. All uncertainties are reported as 95% confidence interval (95% CI; 2σ).

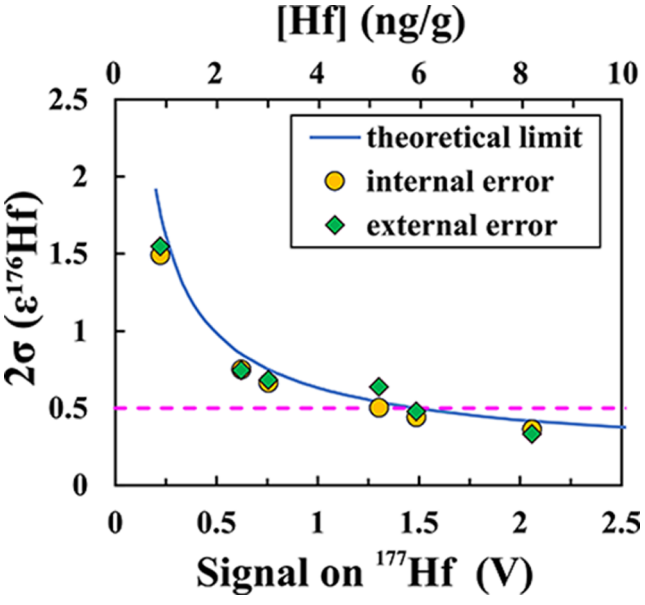

Figure 4. Measurement uncertainties (2σ) of ε^{176}Hf as a function of ^{177}Hf signal intensity (bottom x-axis) and corresponding Hf concentration in the measured solutions (top x-axis) at a sensitivity of 0.22 V for ^{177}Hf (18.60% isotopic abundance) per ppb Hf with a sample uptake rate of ~100 μL/min measured for 10 min. The solid blue line is the theoretically achievable precision on ε^{176}Hf considering counting statistics and Johnson noise (eq 6; Dauphas et al.[60]). The internal and external errors from actual measurements agree well with the theoretically achievable precision, which demonstrates that the current instrumental setup is optimized for Hf isotope measurements. To achieve a precision of better than ~±0.5 on ε^{176}Hf (dashed line) requires analysis of 20 ng Hf, which corresponds to a zircon of 94 μm in diameter.

https://doi.org/10.1021/acsearthspacechem.3c00093
ACS Earth Space Chem. 2024, 8, 36−53

Table 2. Zircon Reference Materials Analyzed in This Study

sample	Hf (ng)	$^{176}Hf/^{177}Hf$	±2σ	$^{178}Hf/^{177}Hf$	±2σ	$\Delta\varepsilon^{176}Hf$[a]	±2σ
AS3	3	0.282206	14	1.467166	26	0.80	0.48
AS3	3	0.282221	13	1.467186	39	1.30	0.45
AS3	10	0.282193	29	1.467173	25	0.32	1.04
AS3	10	0.282194	10	1.467175	19	0.36	0.37
AS3	8	0.282203	14	1.467166	14	0.67	0.51
AS3	8	0.282196	8	1.467174	20	0.43	0.28
AS3	18	0.282200	43	1.467188	133	0.55	1.53
AS3	18	0.282197	5	1.467170	15	0.46	0.19
AS3	20	0.282196	6	1.467181	12	0.44	0.21
AS3	28	0.282198	4	1.467179	11	0.49	0.14
mean AS3		**0.282200**	**5**	**1.467176**	**5**	**0.58**	**0.17**
FC-1[b]		**0.282184**	**8**				
91500	3	0.282317	20	1.467175	55	0.38	0.72
91500	3	0.282327	20	1.467174	27	0.74	0.70
91500	10	0.282312	8	1.467177	23	0.22	0.29
	10	0.282308	13	1.467183	21	0.08	0.45
91500	8	0.282304	5	1.467179	16	−0.08	0.18
91500	18	0.282310	4	1.467176	16	0.14	0.15
91500	20	0.282308	4	1.467174	14	0.09	0.13
91500	28	0.282306	4	1.467179	8	0.01	0.13
mean 91500		**0.282312**	**5**	**1.467177**	**2**	**0.20**	**0.17**
91500		**0.282306**	**4**				
NZ32a	3	0.282157	19	1.467162	50	0.59	0.68
NZ32a	3	0.282143	29	1.467171	25	0.10	1.03
NZ32a	10	0.282128	36	1.467175	37	−0.42	1.29
NZ32a	8	0.282131	9	1.467158	11	−0.33	0.33
NZ32a	18	0.282137	5	1.467167	12	−0.11	0.19
NZ32a	20	0.282134	4	1.467162	11	−0.22	0.14
NZ32a	28	0.282135	3	1.467166	8	−0.17	0.12
mean NZ32a		**0.282138**	**7**	**1.467166**	**4**	**-0.08**	**0.24**
NZ32a		**0.282140**	**5**	**1.467295**	**15**		

[a] $\Delta\varepsilon^{176}Hf = [(^{176}Hf/^{177}Hf_{measured})/(^{176}Hf/^{177}Hf_{literature}) - 1] \times 10^4$. [b] AS3 is from the same geological unit as FC-1.

RESULTS AND DISCUSSION

Limits on Precision of Hf Isotopic Analyses. We discuss below the precision that we were able to achieve and compare the results with what is theoretically possible. The floor to attainable precision by MC-ICP-MS equipped with traditional resistor-based signal amplification is set by counting statistics and Johnson (thermal) noise. Temperature, amplifier gain, and total number of ions captured in the Faraday cups all influence the theoretically attainable precision. Dauphas et al.[60] calculated this theoretical limit for internally normalized ratios and the formula for $^{176}Hf/^{177}Hf$ ratio internally normalized using $^{179}Hf/^{177}Hf$ ratio is,

$$\sigma(\varepsilon^{176}Hf)^2 = 10^8\left[X_{176} + \left(\frac{\mu_{176/177}}{\mu_{179/177}}\right)^2 X_{179} + \left(\frac{\mu_{176/179}}{\mu_{179/177}}\right)^2 X_{177}\right] \quad (6)$$

where

$$X_i = \frac{eR_i}{U_i t} + \frac{4k_B T R_i}{U_i^2 t} \quad (7)$$

$$\mu_{j/i} = \ln(j/i) \quad (8)$$

with $e = 1.602 \times 10^{-19}$ C the elementary charge, $t(s)$ the duration of data acquisition, k_B (m^2 kg s^{-2} K^{-1}) the Boltzmann constant, T(K) the temperature of the feedback resistor, R_i (Ω) is the feedback-resistance of the amplifier used to measure mass i, and U_i is the average voltage measured for mass i. The total acquisition time for a single bracket analysis (30 cycles) was 251.67 s. The sensitivity of the instrument for Hf was 1.2 V/ppb (the voltage corresponds to the sum of the Hf isotopes), which we can use to calculate the voltages for all isotopes for a given Hf concentration in solution. This can also be converted to an amount of Hf consumed by multiplying the Hf solution concentration by the time and nebulizer flow rate of 100 μL/min. The amplifiers are maintained at a temperature of 40 °C and ^{176}Hf, ^{177}Hf, ^{178}Hf, ^{179}Hf, ^{180}Hf isotopes were measured using 10^{11} Ω resistors. We used eq. 6 to calculate the theoretical limit on precision and compared it with the standard deviation calculated from the multiple standard brackets (external precision hereafter). We also compared it with the internal precision calculated by taking the standard deviation of the mean (and, therefore, SE) for all cycles acquired during a single analysis.

Figure 4 shows the theoretically attainable precision curve (solid blue line) on $\varepsilon^{176}Hf$ together with the measured internal and external precision. As expected, the uncertainty increases with lower Hf concentration. The measured internal and external uncertainties agree well with the theoretically achievable precision, which demonstrates that the uncertainties

https://doi.org/10.1021/acsearthspacechem.3c00093
ACS Earth Space Chem. 2024, 8, 36−53

are only limited by counting statistics and detector noise, and the amount of Hf available. At the beginning of each analytical session involving the analysis of precious extraterrestrial samples, we used the first day of measurements to test whether the precision achieved was close to the theoretical limit.

Accuracy of Hf Isotopic Analyses. To test the accuracy of the complete analytical procedure, we performed multiple analyses of three dissolved natural zircon reference materials (AS3, 91500) and one dissolved synthetic zircon doped with REE (MUNZirc 32a) (Table 2). All measurements were done with relatively low amounts of Hf, which did not exceed 20 ng, corresponding to an ~94 μm equivalent zircon grain diameter (calculated assuming ~1 wt% Hf in zircon). Figure 5 shows the difference (expressed in $\Delta\varepsilon^{176}\mathrm{Hf} = \left[\frac{(^{176}\mathrm{Hf}/^{177}\mathrm{Hf})_{\mathrm{measured}}}{(^{176}\mathrm{Hf}/^{177}\mathrm{Hf})_{\mathrm{Literature}}} - 1\right] \times 10^4$) of these three zircons relative to recommended literature $^{176}\mathrm{Hf}/^{177}\mathrm{Hf}$ values of 0.282184 ± 0.000016 for FC-1 (zircon from the same geological unit of AS3), 0.282306 ± 0.000008 for 91500, and 0.282140 ± 0.000005 for MUNZirc 32a (2SD).[54,61] The different data points are replicate analyses involving the whole purification procedure, starting from the same solution but processing different amounts of Hf through chromatography. All data points of 91500, and MUNZirc 32a fall within the error of their expected literature values, meaning that our methodology yields accurate analyses down to 3 ng of total Hf consumed. The $^{176}\mathrm{Hf}/^{177}\mathrm{Hf}$ value that we measure for AS3 is larger than the reference value by ~+0.5 ε,[61] independently of sample size (^{177}Hf signal). This small, but statistically significant discrepancy is unlikely due to unresolved mass interferences because the analyses of MUNZirc 32a are accurate despite the much higher concentrations of potentially interfering elements in that reference material.[54] The difference in $^{176}\mathrm{Hf}/^{177}\mathrm{Hf}$ ratio is more likely due to heterogeneity between the FC-1 sample measured by Woodhead and Hergt[61] and our AS3 zircons.

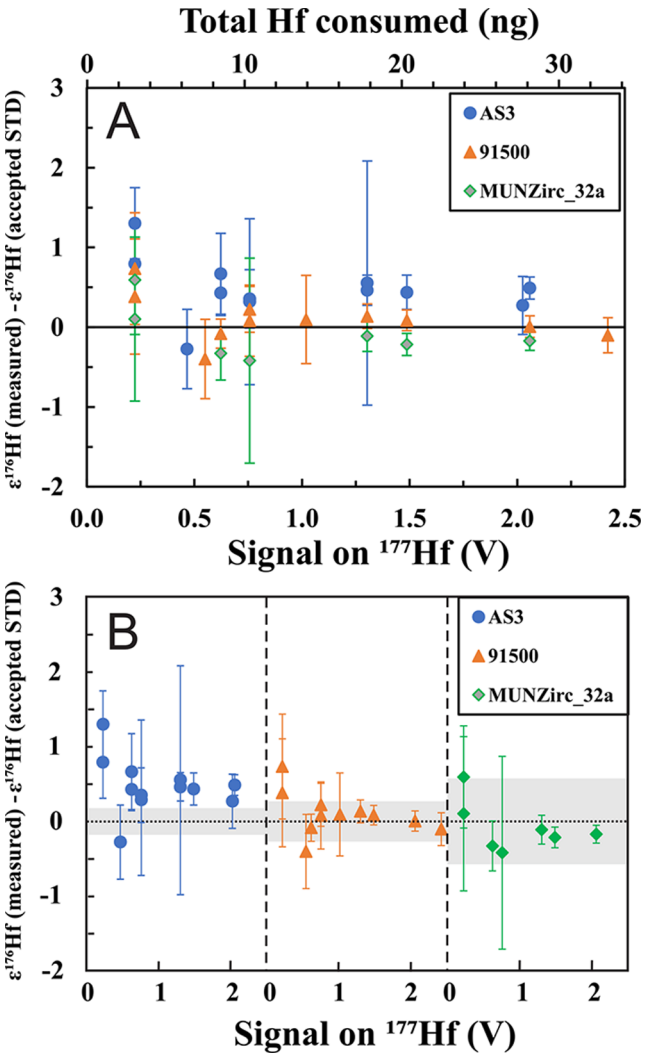

Figure 5. Relative difference from the literature $\varepsilon^{176}\mathrm{Hf}$ values[54,61] of three zircon references (AS3, 91500, and MUNZirc 32a) as a function of ^{177}Hf signal intensity (Table 2). The error bars in panel A are using our measurement errors only. Panel B shows those errors together with those reported for the reference values in the literature (gray bands). There is good agreement between measured and recommended $\varepsilon^{176}\mathrm{Hf}$ values at all solution Hf concentrations (signal on ^{177}Hf), except possibly for AS3 but the literature value is for FC1, which are zircons from the same geological unit but extracted and processed at a different time. Each data point corresponds to a whole-chemistry replicate (involving the whole purification procedure, starting from the same solution but processing different amounts of Hf through chromatography).

Having established that the measurements are accurate and that precision follows the theoretical limit imposed by counting statistics and Johnson noise, we can estimate the precision attainable for samples from different planetary bodies. The developed method would allow us to measure $\varepsilon^{176}\mathrm{Hf}$ in typical extraterrestrial zircons with precisions of ± 1 ε in ~50 μm-size zircons.

Extraterrestrial Test Materials. Interpretation of measured $\varepsilon^{176}\mathrm{Hf}$ in zircons that have been independently dated using U−Pb requires consideration of *in situ* production of ^{176}Hf from ^{176}Lu decay and comparison with CHUR. Knowing the initial $\varepsilon^{176}\mathrm{Hf}$ values and ages of the zircons, it is possible to calculate model ages of crustal differentiation, as enriched reservoirs are characterized by low Lu/Hf ratio and thus unradiogenic $\varepsilon^{176}\mathrm{Hf}$ values.[57] With extraterrestrial samples, additional complications arise from the fact that isotopic ratios can be modified by interaction with cosmic rays, and nucleosynthetic anomalies may be present.

Nucleosynthetic anomalies reflect the fact that the solar system was never fully homogenized and different planetary bodies received different proportions of products of stellar nucleosynthesis.[62,63] The search for nucleosynthetic anomalies in planetary materials has focused on isotopes other than ^{176}Hf because decay of ^{176}Lu obscures potential nucleosynthetic effects on ^{176}Hf.[42,64,65] Sprung et al.[66] evaluated the effect of nucleosynthetic heterogeneities on the ^{176}Lu−^{176}Hf system. They measured several bulk meteorites, and the only isotopic variations that they found were cosmogenic in nature, with no evidence for a distinct nucleosynthetic contribution. They did find hints for the presence of nucleosynthetic anomalies in meteoritic refractory inclusions, corresponding to possible inherited $\varepsilon^{176}\mathrm{Hf}$ variations of up to ~1.5 ε. More meteorite Hf isotope measurements have been performed since the Sprung et al.[66] study that have revealed isotopic anomalies in acid leachates[42,64,65] and refractory inclusions,[41] but no anomaly in bulk rocks.[41,66] Cosmogenic and nucleosynthetic effects form almost orthogonal trends in $\varepsilon^{180}\mathrm{Hf}$–$\varepsilon^{178}\mathrm{Hf}$ space (Figure 6, Sprung et al.[66]), so we can combine those measurements with the known slopes imparted by cosmogenic and nucleosynthetic[42,64,65] effects to estimate the range of allowable nucleosynthetic $\varepsilon^{180}\mathrm{Hf}$ and $\varepsilon^{178}\mathrm{Hf}$ variations in meteorites

https://doi.org/10.1021/acsearthspacechem.3c00093
ACS Earth Space Chem. 2024, 8, 36−53

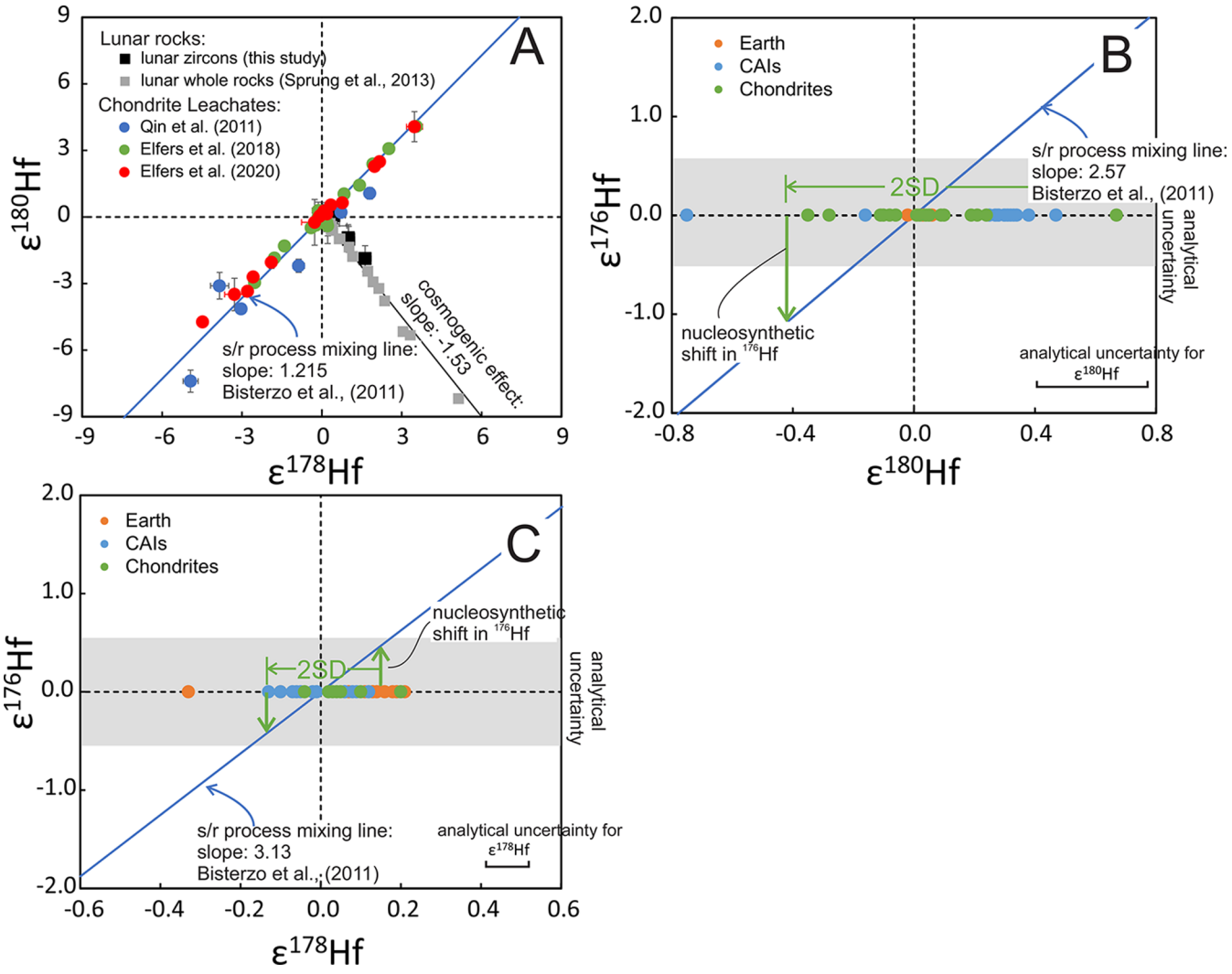

Figure 6. Nucleosynthetic isotopic variation of Hf in chondrites, chondrite leachates, CAIs, and terrestrial rocks. Panel A shows ε^{178}Hf vs ε^{180}Hf for chondrite leachates[42,64,65] and lunar zircons (this study) and lunar whole rocks.[21] The chondrite leachates follow the s/r-process mixing line with a positive slope,[68] while lunar rocks sit on an almost perpendicular trend of cosmogenic effect with a negative slope. To constrain the nucleosynthesis effect on ε^{176}Hf, the ε^{180}Hf and ε^{178}Hf values of chondrites, CAIs and terrestrial rocks are projected onto the s/r process mixing line. Bulk chondrites show no resolvable nucleosynthetic anomalies in ε^{180}Hf (B) and ε^{178}Hf (C), which limits heterogeneities of nucleosynthetic origin on ε^{176}Hf in bulk planetary objects to less than ~±0.3.

(subscript n stands for original nucleosynthetic signature corrected for cosmogenic effects),

$$\varepsilon^{178}\mathrm{Hf}_n = \frac{(\varepsilon^{180}\mathrm{Hf}_m - s_{c,180/178}\varepsilon^{178}\mathrm{Hf}_m)}{(s_{n,180/178} - s_{c,180/178})} \quad (9)$$

$$\varepsilon^{180}\mathrm{Hf}_n = s_{n,180/178}\varepsilon^{178}\mathrm{Hf}_n \quad (10)$$

where $\varepsilon^{178}\mathrm{Hf}_m$ and $\varepsilon^{180}\mathrm{Hf}_m$ are the measured compositions, $s_{n,180/178} = -1.215$ and $s_{c,180/178} = -1.53$ are the slopes between ε^{180}Hf and ε^{178}Hf imparted by nucleosynthetic and cosmogenic effects, respectively. We can then use those compositions to estimate the possible nucleosynthetic shift in ^{176}Hf,

$$\Delta\varepsilon^{176}\mathrm{Hf}_n = s_{n,176/178}\varepsilon^{178}\mathrm{Hf}_n \quad (11)$$

$$\Delta\varepsilon^{176}\mathrm{Hf}_n = s_{n,176/180}\varepsilon^{180}\mathrm{Hf}_n \quad (12)$$

with $s_{n,176/178} = -3.13$ and $s_{n,176/180} = -2.57$, as derived from s-process calculations using the formula of Dauphas et al.[60,67] and data from Bisterzo et al.[68] In Figure 6, we plot the expected relationship between nucleosynthetic anomalies (eqs 9, 10, 11 and 12), together with measurement-derived nucleosynthetic shifts in ε^{178}Hf and ε^{180}Hf. As shown, ε^{178}Hf gives the tightest constraint on the nucleosynthetic contribution on ε^{176}Hf and given the lack of isotopic anomalies for meteorites at a bulk scale, we expect the effect of nucleosynthetic anomalies on ε^{176}Hf to be significantly less than ± 0.3 ε, which is small compared to isotopic variations arising from ^{176}Lu decay. The Moon is known to have very similar isotopic composition to Earth (Dauphas and Schauble[63] and references therein), so the Moon should have started with a Hf isotopic composition almost identical with the terrestrial composition. Therefore, we can neglect any potential isotopic shift due to inherited anomalies.

A more important consideration in ^{176}Lu–^{176}Hf analyses of extraterrestrial samples is the presence of cosmogenic effects produced by cosmic ray exposure both at the surface of the object and during transit to Earth in the case of meteorites. Hafnium isotopes in terrestrial samples are not significantly affected by cosmic rays because Earth's surface is partly shielded by the atmosphere and magnetosphere and rocks at Earth's

https://doi.org/10.1021/acsearthspacechem.3c00093
ACS Earth Space Chem. 2024, 8, 36−53

Table 3. Hf Isotopic Compositions and $^{207}Pb-^{206}Pb$ Ages of Five Lunar Zircons[a]

samples	$^{176}Hf/^{177}Hf$	2σ[b]	$^{178}Hf/^{177}Hf$	2σ[b]	$^{180}Hf/^{177}Hf$	2σ[b]	$^{176}Lu/^{177}Hf$	2σ	t Ma	2σ
14163 Z89 R	0.280077	0.000023	1.467406	0.000034	1.886312	0.000110	0.000822	0.000028	4295.9	0.8
14163 Z9_L1	0.280117	0.000023	1.467192	0.000034	1.886651	0.000110	0.001958	0.000071	4268.3	2.4
14163 Z26_L1	0.280062	0.000023	1.467316	0.000034	1.886476	0.000110	0.000648	0.000022	4337.1	30.3
14163 Z26_L2	0.280037	0.000023	1.467314	0.000034	1.886489	0.000110	0.000619	0.000012	4255.7	16.2
14321 Z3_L1	0.280087	0.000009	1.467183	0.000014	1.886674	0.000098	0.001496	0.000240	4220.5	0.6
14321 Z3_L2	0.280092	0.000014	1.467185	0.000063	1.886687	0.000101	0.002074	0.000091	4217.5	0.5
72275 Z1_L1	0.280017	0.000014	1.467201	0.000063	1.886606	0.000101	0.000902	0.000041	4331.6	3.3
72275 Z1_L2	0.280008	0.000014	1.467234	0.000063	1.886678	0.000101	0.000868	0.000097	4336.2	2.1
72275 Z1 R	0.280004	0.000023	1.467220	0.000034	1.886661	0.000110	0.001000	0.000026	4336.8	0.5

[a]L1 and L2 refer to the first and second leachate, while R refers to residues. [b]Errors reported here are based on the external reproducibilities of the JMC-475 Hf standard.

surface are constantly eroded. To illustrate how cosmogenic effects can be tackled, we have studied 5 lunar zircons. The zircons that we targeted are small and the measurements have relatively low precision. The zircon grains were hand-picked from samples recovered by the Apollo missions: lunar soil 14163, fragmental polymict breccia 72275, and clast-rich breccia 14321. The zircons range in size from 150 to 300 μm, which is on the lower end of the size distribution for lunar zircons studied thus far. They were chemically abraded using the technique outlined in Barboni et al.[2] and references therein (Figure 1). Zircon fragments were removed from epoxy mounts and thermally annealed by transferring the fragments into quartz crucibles and heating to 900 °C for 48 h. Fragments were then rinsed with acetone in 3-mL fluoropolymer PFA beakers, leached in 6 M HCl at 100 °C for one hour, and rinsed again using milliQ H_2O. The zircon fragments were then loaded into 200 μL Savillex "micro"-capsules with 100 μL 29 M HF + 15 μL 3 M HNO_3 for a first step of chemical abrasion[69] in Parr bombs at 185 °C for 6 h. Grains were rinsed 10 times after the 6-h step-1 leaching with 6 M HCl, milliQ H_2O, and 29 M HF before being loaded again into microcapsules with 100 μL 29 M HF + 15 μL 3 M HNO_3 for a second 6-h step of leaching at 185 °C. All the rinses from each zircon were collected in a separate Teflon beaker as leachate L1. The same rinsing procedure as was done for step-1 leaching was also applied after step-2 leaching (saved as L2 for each zircon). The remaining zircon fragments (subsequently referred to as "residues") were then spiked and dissolved to completion in 100 μL 29 M HF + 15 μL 3 M HNO_3 in Parr bombs at 210 °C for 48 h. Leachate L1, L2 and zircon fragment residues were spiked with the EARTHTIME $^{202}Pb-^{205}Pb-^{233}U-^{235}U$ tracer and allowed to equilibrate either on a hotplate (L1 and L2) or during dissolution (residues).[70,71] The dissolved residue and leachates L1 and L2 were individually dried down and converted to chlorides by overnight redissolution using 200 μL of 6N HCl on a hotplate. They were subsequently dried down and brought up in 50 μL of 3 M HCl. Those dry-down and redissolution steps ensure complete sample-spike equilibration. The U−Pb and trace element (including Lu and Hf) fractions were separated by anion exchange column chromatography using a single 50 μL column and AG-1 X8 resin (200−400 mesh; Cl-form) from Eichrom.[72] This procedure involves elution of Zr, Hf and other trace elements in ∼200 μL 3N HCl, which was aliquoted in equal parts and saved for Hf isotopic analysis by MC-ICP-MS and trace element (including Lu/Hf ratio) analysis by single-collector ICP-MS. The U−Pb elutions were collected in single beakers, dried down with a drop of 0.02 M H_3PO_4, and were analyzed on a single outgassed zone-refined Re filament in Si-gel emitter[73] using an Isotopx Phoenix TIMS at Princeton University. For most zircons, we analyzed several leachate fractions and the residue, so the five zircons yielded nine ages and nine $\varepsilon^{176}Hf$ measurements (Tables 3 and S3).

Correction for Radiogenic Ingrowth, Neutron Capture Effects, and Normalization to CHUR. In each zircon, $\varepsilon^{176}Hf$ is first corrected for neutron capture (NC) effects,[2,21,22,66] which mainly change the $^{179}Hf/^{177}Hf$ ratio used for mass bias correction through $^{177}Hf(n,g)^{178}Hf$ and $^{178}Hf(n,g)^{179}Hf$ reactions. Neutron capture effects on $^{176}Hf/^{177}Hf$ (including those arising indirectly from the mass bias correction) are corrected for by monitoring variations in internally normalized $^{178}Hf/^{177}Hf$ and $^{180}Hf/^{177}Hf$ ratios.[2,21,22,66] Our correction procedure builds on the work of Sprung et al.,[21,66] who studied neutron capture effects on Hf and Sm isotopes in lunar samples. The different Hf isotopes are affected differently by thermal (<0.5 eV) and epithermal (>0.5 eV) secondary neutrons because of isotope specific neutron capture cross sections and resonance integrals. The neutron energy distribution can vary depending on target composition, and to a lesser extent depth and irradiation geometry. The $\varepsilon^{180}Hf/\varepsilon^{149}Sm$ ratio provides a sensitive measure of the ratio of epithermal-to-thermal neutron fluences (ep/th) because $\varepsilon^{180}Hf$ is mostly affected by epithermal neutrons while $\varepsilon^{149}Sm$ is mostly affected by thermal neutrons. Sprung et al.[21] adjusted the epithermal and thermal neutron capture fluences in each sample to reproduce the measured $\varepsilon^{180}Hf/\varepsilon^{149}Sm$ ratio. Because thermal neutron capture cross sections and resonance integrals are relatively well determined for Hf isotopes, with knowledge of the ep/th neutron fluence, it is possible to calculate the corresponding cosmogenic shift in $\varepsilon^{176}Hf$. Measuring Sm or Gd isotope ratios in small single lunar zircon grains is difficult if not impossible (a lunar zircon would typically contain only ∼4 pg of Sm and ∼16 pg of Gd), so Barboni et al.[2] used the correlation between calculated cosmogenic $\varepsilon^{176}Hf$ and measured $\varepsilon^{178}Hf$ shifts to correct their data for neutron capture effects. Using combined Sm and Hf isotopic analyses of low- and high-Ti lunar basalts and KREEP-rich samples, Sprung et al.[21] showed that there is a tight correlation between shifts in $\varepsilon^{180}Hf$ and $\varepsilon^{178}Hf$ and that this correlation is insensitive to varying ep/th neutron exposure spanning a range from 0.44 to 2.2 (determined from $\varepsilon^{149}Sm$). This suggests that cosmogenic shifts in Hf isotopic compositions are not very dependent on the neutron energy distribution (ep:th ratio) and that either $\varepsilon^{180}Hf$ or $\varepsilon^{178}Hf$ can be monitored to quantify the cosmogenic correction on $\varepsilon^{176}Hf$ arising either directly from n-capture on ^{176}Hf and ^{177}Hf or indirectly via the mass bias correction (i.e., $^{179}Hf/^{177}Hf$).

https://doi.org/10.1021/acsearthspacechem.3c00093
ACS Earth Space Chem. 2024, 8, 36−53

Because cosmogenic shifts on $^{176}Hf/^{177}Hf$ can amount to several ε units, we have re-evaluated the effect of variations in the energy spectrum of secondary neutrons to compare with the model results of Sprung et al.[21] We consider thermal cross sections and resonance integrals taken from the Jeff-3.1 database[74,75] and test whether our results depend on the choice of the nuclear database by comparing it with cross-sections and resonance integrals from the ENDFB-VIII database.[76] It turns out that the calculated cosmogenic shifts are essentially indistinguishable. Our calculations confirm that calculated $\Delta\varepsilon^{176}Hf/\Delta\varepsilon^{178}Hf$ and $\Delta\varepsilon^{176}Hf/\Delta\varepsilon^{180}Hf$ vary little with the ratio ep/th (Figure 7). For pure thermal neutrons (ep/th = 0), we have $\Delta\varepsilon^{176}Hf/\Delta\varepsilon^{178}Hf = 2.063$ and $\Delta\varepsilon^{176}Hf/\Delta\varepsilon^{180}Hf = -1.687$. For pure epithermal neutrons (ep/th = $+\infty$), we have $\Delta\varepsilon^{176}Hf/\Delta\varepsilon^{178}Hf = 2.368$ and $\Delta\varepsilon^{176}Hf/\Delta\varepsilon^{180}Hf = -1.527$.

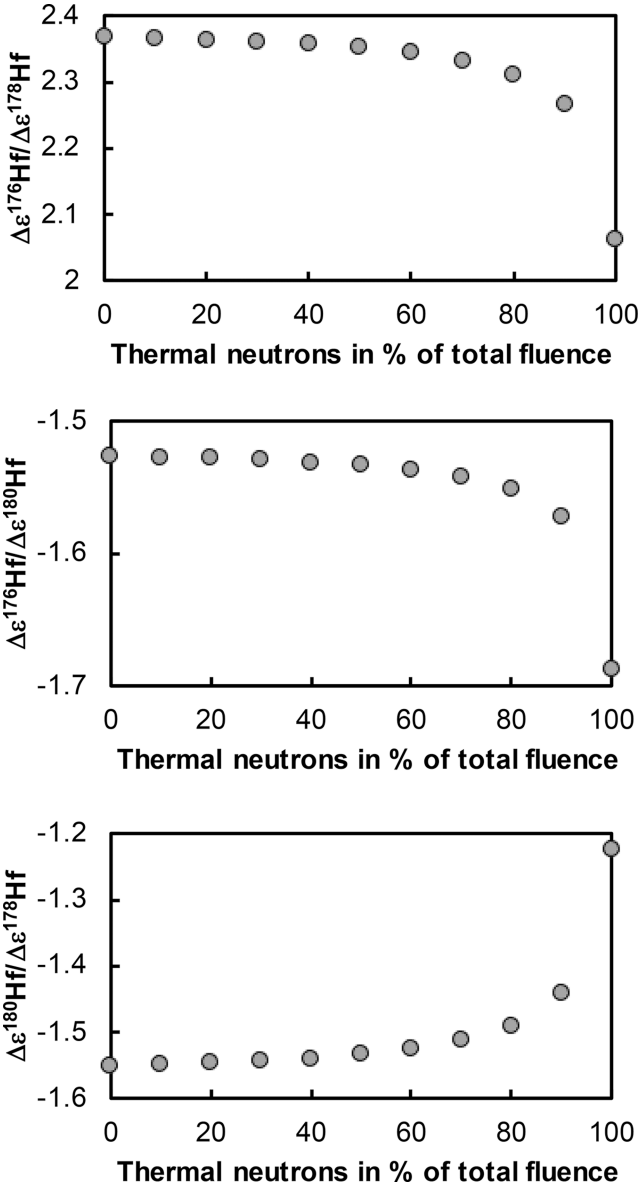

Figure 7. Ratio of neutron capture induced Hf isotopic shifts $\Delta\varepsilon^{176}Hf/\Delta\varepsilon^{178}Hf$, $\Delta\varepsilon^{176}Hf/\Delta\varepsilon^{180}Hf$, and $\Delta\varepsilon^{180}Hf/\Delta\varepsilon^{178}Hf$ as a function of fraction of thermal neutrons in the total neutron fluence. Previous work has shown that the proportion of thermal neutrons is 30 −70% of the total fluence.[21]

With ep/th in the range 0.44 to 2.2 documented by Sprung et al.,[21] $\Delta\varepsilon^{176}Hf/\Delta\varepsilon^{178}Hf$ ranges from 2.332 to 2.361 and $\Delta\varepsilon^{176}Hf/\Delta\varepsilon^{180}Hf$ ranges from −1.542 to −1.530. The ratio $\Delta\varepsilon^{180}Hf/\Delta\varepsilon^{178}Hf$ varies little with the fractions of thermal and epithermal neutrons (∼−1.53 for ep/th ratios relevant to lunar samples), so this is not a basis to prefer either $\Delta\varepsilon^{178}Hf$ or $\Delta\varepsilon^{180}Hf$ for neutron-capture correction on $\varepsilon^{176}Hf$. The observed slope $\Delta\varepsilon^{180}Hf/\Delta\varepsilon^{178}Hf$ in lunar samples is −1.58 (Sprung et al.,[21] this study), which is close to our theoretically predicted slope of −1.53. For comparison, the calculations presented in Sprung et al.[21] yield $\Delta\varepsilon^{176}Hf/\Delta\varepsilon^{178}Hf = 2.613$, $\Delta\varepsilon^{176}Hf/\Delta\varepsilon^{180}Hf = -1.652$, and $\Delta\varepsilon^{180}Hf/\Delta\varepsilon^{178}Hf = -1.58$. Estimating systematic errors introduced by model calculations of cosmogenic effects is difficult and we take the differences between the slopes inferred by Sprung et al.[21] and ours as a measure of uncertainty. We, therefore, have $\Delta\varepsilon^{176}Hf/\Delta\varepsilon^{178}Hf = 2.35 \pm 0.25$ (±11%) and $\Delta\varepsilon^{176}Hf/\Delta\varepsilon^{180}Hf = -1.54 \pm 0.11$ (±7%). The fact that model predictions match the measured $\Delta\varepsilon^{180}Hf/\Delta\varepsilon^{178}Hf$ ratio within ∼3% strengthens the view that model predictions are accurate. To further assess the reliability of the correction for cosmogenic effects on ^{176}Hf, we apply both $\Delta\varepsilon^{178}Hf$ and $\Delta\varepsilon^{180}Hf$ corrections and compare the two (the c subscript stands for corrected for cosmogenic effects and p stands for present measured value),

$$\varepsilon^{176}Hf_{zrc-p,c} = \varepsilon^{176}Hf_{zrc-p} - \alpha_i\varepsilon^{i}Hf_{zrc} \quad (13)$$

We can also write this correction for absolute ratios using the approximation $\varepsilon^{176}Hf_{zrc-p,c} - \varepsilon^{176}Hf_{zrc-p} \approx 10^4[(^{176}Hf/^{177}Hf)^*_{zrc-p,c}/(^{176}Hf/^{177}Hf)^*_{zrc-p} - 1]$,

$$\left(\frac{^{176}Hf}{^{177}Hf}\right)^*_{zrc-p,c} = \left(\frac{^{176}Hf}{^{177}Hf}\right)^*_{zrc-p}\left(1 - \frac{\alpha_i\varepsilon^{i}Hf}{10^4}\right) \quad (14)$$

where $\alpha_i = 2.35$ for $i = 178$ and $\alpha_i = -1.54$ for $i = 180$.

We also apply the correction given by Sprung et al.[21] and compare the results with our updated formulas (Table 4). The lunar zircons analyzed in this study have $\varepsilon^{178}Hf$ values that vary between ∼0 and 2, and $\varepsilon^{180}Hf$ values that vary between ∼0 and −2. Table 4 shows how the different corrections compare to each other for our data set. The corrections on $\varepsilon^{176}Hf$ using $\varepsilon^{178}Hf$ or $\varepsilon^{180}Hf$ and the model predictions from either Sprung et al.[21] or the present work show some scatter, but we see no systematic offset between the corrections, suggesting that much of the uncertainty in the correction stems from the precision with which the cosmogenic shifts are measured.

Correction for the decay of ^{176}Lu into ^{176}Hf after zircon crystallization is done by combining TIMS high-precision U−Pb crystallization ages and measured Lu/Hf ratios. TIMS U−Pb dating was done at Princeton University using established procedures.[2,77] The U−Pb age was calculated for each leachate and trace elements (including Lu/Hf ratio) were analyzed on an aliquot of each solution using a Thermo iCAP single collector quadrupole ICP-MS following the methodology in O'Connor et al.[78] Measurements were calibrated using a matrix-matched external calibration solution with Lu, Hf, and other trace elements proportional to those in natural zircon. Instrument drift and data reproducibility were monitored by the measurement of four independent standard solutions: MUNZirc 1−2c, MUNZirc 3−2c, Plesovice,[54,79] and an in-house Zr−Hf standard. The initial zircon $^{176}Hf/^{177}Hf$ ratio corrected for both cosmogenic effects and ^{176}Lu decay is

https://doi.org/10.1021/acsearthspacechem.3c00093
ACS Earth Space Chem. 2024, 8, 36−53

Table 4. Comparisons between the Single Zircon Neutron Capture Induced $\varepsilon^{176}Hf_{CHUR}$ Shifts Using Different Methods and Models

	$\Delta\varepsilon^{176}Hf/^{177}Hf$			
	Sprung theoretical model		This study	
samples	based on $\varepsilon^{178}Hf/^{177}Hf$	based on $\varepsilon^{180}Hf/^{177}Hf$	based on $\varepsilon^{178}Hf/^{177}Hf$	based on $\varepsilon^{180}Hf/^{177}Hf$
14163 Z89 R	−4.24	−3.10	−3.82	−2.89
14163 Z9_L1	−0.43	−0.13	−0.39	−0.12
14163 Z26_L1	−2.63	−1.66	−2.37	−1.55
14163 Z26_L2	−2.59	−1.55	−2.33	−1.44
14321 Z3_L1	−0.26	0.07	−0.23	0.07
14321 Z3_L2	−0.30	0.18	−0.27	0.17
72275 Z1_L1	−0.59	−0.52	−0.53	−0.49
72275 Z1_L2	−1.18	0.11	−1.06	0.10
72275 Z1 R	−0.93	−0.04	−0.84	−0.04

$$\left(\frac{^{176}Hf}{^{177}Hf}\right)_{zrc-t,c} = \left(\frac{^{176}Hf}{^{177}Hf}\right)_{zrc-p}\left(1 - \frac{\alpha_i\varepsilon^i Hf}{10^4}\right) - \left(\frac{^{176}Lu}{^{177}Hf}\right)_{zrc-p}\left(e^{\lambda_{^{176}Lu}t} - 1\right) \quad (15)$$

The time t represents the crystallization age of the zircon given by isotopic closure of the U/Pb system, which is assumed to be equivalent to that for Lu/Hf. The main uncertainty with this correction lies in the measured Lu/Hf ratio as any systematic error in the decay constant does partially cancel out when the Hf isotopic composition is expressed relative to that of the chondritic uniform reservoir (CHUR) at the same time.

A potential concern with data interpretation is whether U−Pb and Lu−Hf systematics measured in a leachate or residue can be reliably linked or if they were decoupled during either residence on the Moon or chemical processing in the laboratory. The chemical abrasion procedure employed for U−Pb dating could have fractionated the Lu/Hf ratio by an incongruent dissolution. Those two systems could also have been decoupled by zoning or Pb loss after metamictisation. One powerful approach for addressing this concern is to compare the calculated initial $\varepsilon^{176}Hf$ values from successive leaching steps and residues. Indeed, zircons with simple single-stage histories are anticipated to exhibit a uniform initial Hf isotopic composition. Variations in initial $\varepsilon^{176}Hf$ values might indicate that the zircon had a complex multistage history, making it unsuitable for dating, or that there was incongruent Lu/Hf dissolution, rendering the age adjustment questionable. Several leaching steps were analyzed in three zircons: 14163 Z26 (L1, L2), 14321 Z3 (L1, L2), and 72275 Z1 (L1, L2, and R). The differences in raw $\varepsilon^{176}Hf$ between the two leaching steps of 14163 Z26 and 14321 Z3 are 0.89 ± 1.16 and 0.18 ± 0.59 ε-units, respectively, which is indistinguishable from zero. The mean square weighted deviation on the three raw $^{176}Hf/^{177}Hf$ ratios measured in 72275 Z1 R is 0.64, when the 2-sided 95% confidence interval for the reduced-χ^2 distribution for $n = 3 - 1 = 2$ degrees of freedom is 0.025 to 3.69, indicating that the three values are identical within their given errors. If the cosmogenic correction is accurate, U−Pb ages have not been disturbed, and Lu and Hf dissolve congruently, we would expect initial $\varepsilon^{176}Hf$ values to remain consistent within error. Not propagating the error on CHUR, the $\varepsilon^{176}Hf$ values are + 0.09 ± 0.96 and −2.63 ± 0.96 for 14163 Z26, −2.17 ± 0.80 and −3.79 ± 1.11 for 14321 Z3, and −0.57 ± 1.02, −1.22 ± 1.06, and −1.53 ± 0.96 for 72275 Z1. A minor discrepancy exists between the two corrected values for 14163 Z26, which might stem from the incongruent dissolution of Lu/Hf. All other values align with each other. Overall, our findings show no clear evidence of disturbance in the coupled Lu−Hf and U−Pb systematics of analyzed zircons. However, given the limited number of measurements in our data set, there remains possibilities that zircons with a complex history could exhibit such disturbances. Therefore, A thorough examination of the initial $\varepsilon^{176}Hf$ values, Lu/Hf ratios, and U−Pb ages from different leachates is recommended to filter out zircons with complex histories.

The CHUR $^{176}Hf/^{177}Hf$ evolution is most accurately calculated based on estimates of the $^{176}Hf/^{177}Hf$ ratio at solar system formation (ss = Solar System Initial) of 0.279781 ± 0.000018 and the present-day chondritic $^{176}Lu/^{177}Hf$ ratio of 0.0338 ± 0.0001[25]

$$\left(\frac{^{176}Hf}{^{177}Hf}\right)_{CHUR-t} = \left(\frac{^{176}Hf}{^{177}Hf}\right)_{CHUR-ss} + \left(\frac{^{176}Lu}{^{177}Hf}\right)_{CHUR-p}\left(e^{\lambda_{^{176}Lu}t_{ss}} - e^{\lambda_{^{176}Lu}t}\right) \quad (16)$$

where CHUR−t, CHUR−ss, and CHUR−p denote CHUR composition at time t before present, at the formation of the solar system, and at present, and t_{ss} is the age of the solar system. We are interested in tracking how the initial $^{176}Hf/^{177}Hf$ isotopic compositions of zircons compare to the CHUR taken at the same time. Because isotopic variations are small, it is customary to express them in $\varepsilon^{176}Hf$ notation $\varepsilon^{176}Hf_t = [(^{176}Hf/^{177}Hf)_t/(^{176}Hf/^{177}Hf)_{STD} - 1] \times 10^4$, where STD denotes a reference material. The standard is usually taken to be CHUR−t. Relative to this reference, the $\varepsilon^{176}Hf_t$ value of zircons can be expressed as

$$\varepsilon^{176}Hf_{zrc-t,c/CHUR-t} = \left[\frac{\left(\frac{^{176}Hf}{^{177}Hf}\right)_{zrc-p}\left(1 - \frac{\alpha_i\varepsilon^i Hf}{10^4}\right) - \left(\frac{^{176}Lu}{^{177}Hf}\right)_{zrc-p}\left(e^{\lambda_{^{176}Lu}t} - 1\right)}{\left(\frac{^{176}Hf}{^{177}Hf}\right)_{CHUR-ss} + \left(\frac{^{176}Lu}{^{177}Hf}\right)_{CHUR-p}\left(e^{\lambda_{^{176}Lu}t_{ss}} - e^{\lambda_{^{176}Lu}t}\right)} - 1\right] \times 10^4 \quad (17)$$

Uncertainties. The uncertainties of $\varepsilon^{176}Hf_{zrc-t,c}$ were propagated by using both analytical and Monte-Carlo methods. The analytical approach can be implemented in a spreadsheet, but it involves making some approximations that can be tested using the Monte-Carlo approach. The parameters in eq 17 that are uncertain are: the measured internally normalized $(^{176}Hf/^{177}Hf)_{zrc-p}$ ratio (x_1), the factor α_i used to correct cosmogenic effects $\alpha_{178} = 2.35 \pm 0.25$ and $\alpha_{180} = -1.54 \pm 0.11$ (x_2), the measured isotopic shifts ε^i Hf in ^{178}Hf or ^{180}Hf that are

https://doi.org/10.1021/acsearthspacechem.3c00093
ACS Earth Space Chem. 2024, 8, 36−53

used to correct cosmogenic effects (x_3), the $(^{176}Lu/^{177}Hf)_{zrc\text{-}p}$ ratio of the zircon used to correct for in situ decay of ^{176}Lu (x_4), the decay constant $\lambda^{176}_{Lu} = 1.867 \pm 0.008 \times 10^{-11}$ Ga^{-1} (x_5[1]), the crystallization age of the zircon t (x_6), the CHUR parameters $(^{176}Hf/^{177}Hf)_{CHUR-ss} = 0.279781 \pm 0.000018$ (x_7) and $(^{176}Lu/^{177}Hf)_{CHUR-p} = 0.0338 \pm 0.0001$ (x_8), and the age of the solar system $t_{ss} = 4567.3 \pm 0.16$ Ma (x_9[80]). As discussed earlier, some of these uncertainties like that on the decay constant largely cancel out when using the $\varepsilon^{176}Hf$ notation normalized to contemporaneous CHUR, but we propagated all uncertainties to evaluate which ones could safely be neglected, and we provide a simplified formula that only considers the ones that matter. Some assumptions/approximations must be made to derive an analytic equation, most notably that the functional relationship can be linearized over the range defined by uncertainties and that the distribution remains approximately Gaussian. To evaluate the accuracy of the analytical approach, we have also run Monte Carlo simulations (MCS) by randomly generating a large number (200000) of multivariate normal distribution for variables x_1, x_2, x_3, x_4, x_5, x_6, x_7, x_8, x_9 based on the quoted values and uncertainties. All uncertainties are taken to be independent, except for the measured $(^{176}Hf/^{177}Hf)_{zrc-p}$ ratio (x_1) on the one hand, and ε^{178} Hf and ε^{180} Hf (x_3) used for correcting cosmogenic effects on the other hand. This correlation in errors arises from taking ratios of all isotopes to ^{177}Hf and applying the same $^{179}Hf/^{177}Hf$ internal normalization scheme to all ratios. The error correlations (correlation coefficients) are calculated based on cycle-level variations. The data involve not only internal normalization but also normalization to bracketing standards, which affects error correlations. This was accounted for using the formulas of Dauphas et al.[81] Details are provided in the Supporting Information. In the MCS, we use a joint binormal probability distribution to generate (x_1, x_3). All other values are assumed to be independent. We also consider the correlation coefficient between x_1 and x_3 in the derivation of the analytical formula. The calculated correlation coefficients (ρ) are compiled in Table S2.

We used two forms of eq 17 to calculate the errors for CHUR-normalized $\varepsilon^{176}Hf$. The first one is eq 17 with the CHUR value as random variable in the denominator, $\varepsilon^{176}Hf_{zrc-t,c/CHUR-t} = f_1(x_1, x_2, x_3, x_4, x_5, x_6, x_7, x_8, x_9)$ with

$$f_1 = \left[\frac{x_1\left(1 - \frac{x_2x_3}{10^4}\right) - x_4(e^{x_5x_6} - 1)}{x_7 + x_8(e^{x_5x_9} - e^{x_5x_6})} - 1\right] \times 10^4 \quad (18)$$

The second expression separates the errors arising from $^{176}Hf/^{177}Hf$ measurements from CHUR parameters. The reasons for doing so are the following: (i) The analytical solution starting with the full expression (eq 18) would be cumbersome to derive and use. (ii) Equation 17 encompasses errors from both sample measurements and CHUR normalization, with the latter a systematic error that affects all zircons and creates a statistical dependency between model ages. This is important if one is interested in examining the statistical distribution of zircon model ages. (iii) Splitting CHUR and zircon uncertainties allows us to partly separate uncertainties from the literature and uncertainties tied to the quality of our measurements.

To split the errors from CHUR and the zircon measurement, we recognize that

$$\begin{aligned}\varepsilon^{176}Hf_{zrc-t,c/CHUR-t} &= \left[\frac{(^{176}Hf/^{177}Hf)_{zrc-t,c}}{(^{176}Hf/^{177}Hf)_{CHUR-t}} - 1\right]10^4 \\ &\simeq \left[\frac{(^{176}Hf/^{177}Hf)_{zrc-t,c}}{(^{176}Hf/^{177}Hf)_{STD}} - 1\right]10^4 - \left[\frac{(^{176}Hf/^{177}Hf)_{CHUR-t}}{(^{176}Hf/^{177}Hf)_{STD}} - 1\right]10^4 \\ &\simeq \varepsilon^{176}Hf_{zrc-t/STD} - \varepsilon^{176}Hf_{CHUR-t/STD} \quad (19)\end{aligned}$$

where STD can be any standard of our choosing. While eqs 17 and 19 yield the same values for $\varepsilon^{176}Hf_{zrc-t,c/CHUR-t}$, the two formulas lead to handling error propagation differently. When propagating errors, eq 17 would treat $X = (^{176}Hf/^{177}Hf)_{zrc-t}$ and $Y = (^{176}Hf/^{177}Hf)_{CHUR-t}$ as random variables in $\varepsilon = (X/Y-1)10^4$ and would introduce dependency in calculated model ages. If we use eq 19 and adopt for the standard the exact value of CHUR $\tilde{Y}$ (the tilde accent is here to indicate that it is not a random variable) at the time of the zircon crystallization, $\varepsilon \simeq (X/\tilde{Y} - 1)10^4 - (Y/\tilde{Y} - 1)10^4$, we separate the components of the uncertainty that lead to interdependency in model ages of individual zircons. In this approach, we have

$$\varepsilon^{176}Hf_{zrc-t,c/\overline{CHUR-t}} = \left[\frac{\left(\frac{^{176}Hf}{^{177}Hf}\right)_{zrc-p}\left(1 - \frac{\alpha_i\varepsilon^i Hf}{10^4}\right) - \left(\frac{^{176}Lu}{^{177}Hf}\right)_{zrc-p}(e^{\lambda_{^{176}Lu}t} - 1)}{\left(\overline{\frac{^{176}Hf}{^{177}Hf}}\right)_{CHUR-ss} + \left(\overline{\frac{^{176}Lu}{^{177}Hf}}\right)_{CHUR-p}(e^{\tilde{\lambda}_{^{176}Lu}\tilde{t}_{ss}} - e^{\tilde{\lambda}_{^{176}Lu}\tilde{t}})} - 1\right] \times 10^4 \quad (20)$$

$$\varepsilon^{176}Hf_{CHUR-t/\overline{CHUR-t}} = \left[\frac{\left(\frac{^{176}Hf}{^{177}Hf}\right)_{CHUR-ss} + \left(\frac{^{176}Lu}{^{177}Hf}\right)_{CHUR-p}(e^{\lambda_{^{176}Lu}t_{ss}} - e^{\lambda_{^{176}Lu}t})}{\left(\overline{\frac{^{176}Hf}{^{177}Hf}}\right)_{CHUR-ss} + \left(\overline{\frac{^{176}Lu}{^{177}Hf}}\right)_{CHUR-p}(e^{\tilde{\lambda}_{^{176}Lu}\tilde{t}_{ss}} - e^{\tilde{\lambda}_{^{176}Lu}\tilde{t}})} - 1\right] \times 10^4 \quad (21)$$

where variables with tilde are exact values with no error. The expected value of $\varepsilon^{176}Hf_{CHUR-t/\overline{CHUR-t}}$ is 0 at all ages. The denominator is no longer a random variable and we note it as

$$C = \overline{(^{176}Hf/^{177}Hf)}_{CHUR-ss} + \overline{(^{176}Hf/^{177}Hf)}_{CHUR-p}(e^{\tilde{\lambda}_{^{176}Lu}\tilde{t}_{ss}} - e^{\tilde{\lambda}_{^{176}Lu}\tilde{t}}).$$

Equations 20−21 can be written as functions f_2 (x_1, x_2, x_3, x_4, x_5, x_6) and f_3 (x_5, x_6, x_7, x_8, x_9) using the variables mentioned above

$$\varepsilon^{176}Hf_{zrc-t,c/\overline{CHUR-t}} = f_2 = \left[\frac{x_1 - x_4(e^{x_5x_6} - 1)}{C} - 1\right] \times 10^4 - \frac{x_1x_2x_3}{C} \quad (22)$$

$$\varepsilon^{176}Hf_{CHUR-t/\overline{CHUR-t}} = f_3 = \left[\frac{x_7 + x_8(e^{x_5x_9} - e^{x_5x_6})}{C} - 1\right] \times 10^4 \quad (23)$$

We note

$$\begin{aligned}&\varepsilon^{176}Hf_{zrc-t,c/\overline{CHUR-t}} - \varepsilon^{176}Hf_{CHUR-t/\overline{CHUR-t}} = f_4 \\ &= \frac{x_1 - x_4(e^{x_5x_6} - 1) - x_7 - x_8(e^{x_5x_9} - e^{x_5x_6})}{C} \times 10^4 - \frac{x_1x_2x_3}{C} \quad (24)\end{aligned}$$

The uncertainties of the various parameters in eqs 22, 23, and 24 can be propagated analytically using the approximation, $\sigma_f^2 \simeq \sum\left(\frac{\partial f}{\partial x_i}\right)^2\sigma_{x_i}^2 + 2\sum\sum\frac{(\partial f)^2}{\partial x_i\partial x_j}\sigma_{x_ix_j}$, where $\sigma_{x_ix_j}$ is the covariance (see Supporting Information for details). A virtue of the analytical approach is that it is easy to quantify the contribution of each variable to the total variance (Table S1). Examination of

https://doi.org/10.1021/acsearthspacechem.3c00093
ACS Earth Space Chem. 2024, 8, 36−53

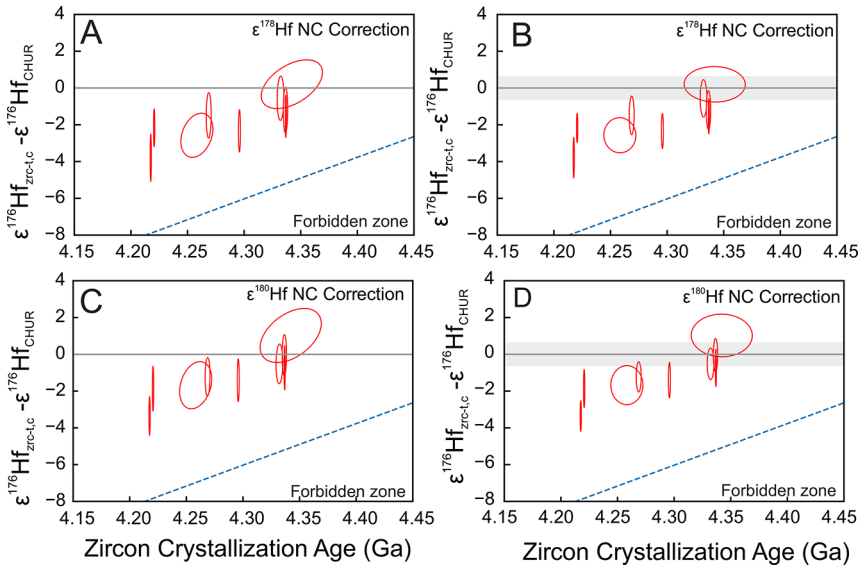

Figure 8. Single zircon initial $^{176}Hf/^{177}Hf$ isotopic composition (expressed as departure from CHUR in ε-unit) as a function of $^{207}Pb/^{206}Pb$ zircon crystallization age calculated using eq 18 (A, C) and eqs 22 and 23 (B, D). The difference between these two approaches is whether CHUR uncertainties are kept separated (gray bands in panels B, D) or not (panels A, C); see text for details. Each zircon $\varepsilon^{176}Hf_{zrc-t,c/CHUR-t}$ value in this study was corrected for neutron capture effects using either $\varepsilon^{178}Hf$ (A, B) or $\varepsilon^{180}Hf$ (C, D) and the theoretically predicted cosmogenic effect correlation. Error ellipses are of 95% confidence level. The dashed line corresponds to a two-stage model evolution for a reservoir with Lu/Hf = 0 isolated from the solar system at 4.567 Ga.

the error budget (Table S1) shows that some uncertainties can be safely neglected, and we can set $\left(\frac{\partial f}{\partial x_i}\right)^2 \sigma_{x_i}^2$ for variables x_2, x_4, x_5, x_6, x_8, and x_9 to 0 without losing too much accuracy in error estimates. Under those conditions, we have

$$\sigma_{f_4}^2 \simeq \left(\frac{10^4}{C}\right)^2\left[\left(1-\frac{x_2x_3}{10^4}\right)^2\sigma_{x_1}^2+\sigma_{x_7}^2\right]+\frac{x_1^2x_2^2}{c^2}\sigma_{x_3}^2 + 2\frac{10^4}{C^2}\left(1-\frac{x_2x_3}{10^4}\right)x_1x_2\sigma_{x_1x_3} \quad (25)$$

These formulas are implemented in an Excel spreadsheet provided as Supporting Information that can be used for data reduction.

Figure 8 shows the results of the five lunar zircons measured here. The final uncertainty of each $\varepsilon^{176}Hf_{zrc-t,c}$ value is calculated by propagating errors resulting from measurements of $^{176}Hf/^{177}Hf$, $^{178}Hf/^{177}Hf$, $^{180}Hf/^{177}Hf$, and $^{176}Lu/^{177}Hf$, and the crystallization age t. In panels A and C, the uncertainties on $\varepsilon^{176}Hf_{zrc-t,c/CHUR-t}$ were calculated using eq 18. The uncertainty ellipse is slanted because of the different age dependencies of $\varepsilon^{176}Hf_{zrc-t,c}$ and $\varepsilon^{176}Hf_{CHUR}$. In this approach, distributions of zircon model ages are potentially less straightforward to interpret as the values of $x_5 = \lambda$, $x_7 = (^{176}Hf/^{177})Hf)_{CHUR-ss}$, $x_8 = (^{176}Lu/^{177}Hf)_{CHUR-p}$, and $x_9 = t_{ss}$ will affect all zircon $\varepsilon^{176}Hf_{zrc-t,c}$–$\varepsilon^{176}Hf_{CHUR}$ analyses, and the data points are not truly independent. In panels B and D, the uncertainties on $\varepsilon^{176}Hf_{zrc-t,c}$ and $\varepsilon^{176}Hf_{CHUR}$ are kept separated through the use of Eqs. 22 and 23. In this approach, the dependence of all individual zircon model ages on shared parameters x_5, x_7, x_8, and x_9 can be considered to calculate model age distributions of zircon populations. The difficulty with this approach is that the dependence of $\varepsilon^{176}Hf_{zrc-t,c}$ and $\varepsilon^{176}Hf_{CHUR}$ on crystallization age is lost, and the individual uncertainty ellipses are less realistic. Both approaches to propagate uncertainties have some pitfalls that can be eliminated in a MCS by randomizing the shared parameters x_5, x_7, x_8, and x_9 for the entire data set, but as discussed below, the two approaches yield almost identical age distributions. Our preferred option is to split uncertainties on $\varepsilon^{176}Hf_{zrc-t,c}$ and $\varepsilon^{176}Hf_{CHUR}$ because (i) it better portrays uncertainties arising from our zircon analyses rather than combining those with uncertainties on CHUR and the decay constant from the literature and (ii) an analytical expression is available to propagate uncertainties.

The main purpose of estimating the initial Hf isotopic compositions of zircons and comparing them with contemporaneous CHUR is to derive model ages of magmatic differentiation. Those model ages are calculated assuming a 2-stage evolution, where a reservoir R evolves with CHUR composition from t_{ss} to t_d before present, and then evolves with a fractionated $(^{176}Lu/^{177}Hf)_{R-p}$ ratio (x_{10}, the p subscript indicates that the $^{176}Lu/^{177}Hf_{Hf}$ ratio of that hypothetical reservoir is expressed as what would be its present-day value) until the zircon crystallizes at t. In that context, the Hf isotopic composition of zircon and reservoir R at time t before the present should be the same,

$$\left(\frac{^{176}Hf}{^{177}Hf}\right)_{zrc-t,c} = \left(\frac{^{176}Hf}{^{177}Hf}\right)_{R-t} = \left(\frac{^{176}Hf}{^{177}Hf}\right)_{R-t_d} + \left(\frac{^{176}Lu}{^{177}Hf}\right)_{R-p}\left(e^{\lambda_{^{176}Lu}t_d} - e^{\lambda_{^{176}Lu}t}\right) \quad (26)$$

The Hf isotopic composition for CHUR at time t is,

$$\left(\frac{^{176}Hf}{^{177}Hf}\right)_{CHUR-t} = \left(\frac{^{176}Hf}{^{177}Hf}\right)_{CHUR-t_d} + \left(\frac{^{176}Lu}{^{177}Hf}\right)_{CHUR-p}\left(e^{\lambda_{^{176}Lu}t_d} - e^{\lambda_{^{176}Lu}t}\right) \quad (27)$$

Using the relationship $(^{176}Hf/^{177}Hf)_{R-t_d} = (^{176}Hf/^{177}Hf)_{CHUR-t_d}$, eqs 26 and 27 can be combined into the following equation,

https://doi.org/10.1021/acsearthspacechem.3c00093
ACS Earth Space Chem. 2024, 8, 36−53

Table 5. Calculated ε^{176}Hf and Model Ages of 5 Lunar Zircons

samples	$\varepsilon^{176}Hf_{zrc-t,c/CHUR-t}$	2σ (Monte Carlo)	2σ (analytical eq)	$\sigma_{f_1}^2$	$\sigma_{f_4}^2$	$\sigma_{f_2}^2$	$\sigma_{f_3}^2$	minimum model age t_d(Ma) $^{176}Lu/^{177}Hf_{R-p} = 0$	2σ (Ma)	model age t_d(Ma) $^{176}Lu/^{177}Hf_{R-p}$ = 0.0153 ± 0.0033	2σ (Ma)
NC-178 correction											
14163 Z89 R	−2.34	1.15	1.15	0.33	0.33	0.23	0.10	4391	47	4470	87
14163 Z9_L1	−1.50	1.23	1.23	0.38	0.38	0.27	0.10	4330	50	4380	98
14163 Z26_L1	0.09	1.37	1.37	0.47	0.47	0.23	0.24	4334	47	4331	99
14163 Z26_L2	−2.63	1.22	1.21	0.37	0.37	0.23	0.14	4363	47	4452	89
14321 Z3_L1	−2.17	1.03	1.03	0.27	0.26	0.16	0.10	4309	42	4383	83
14321 Z3_L2	−3.79	1.29	1.28	0.42	0.41	0.31	0.10	4373	53	4501	96
72275 Z1_L2	−0.57	1.21	1.20	0.37	0.36	0.26	0.11	4355	49	4375	96
72275 Z1_L1	−1.22	1.24	1.24	0.38	0.38	0.28	0.10	4386	51	4427	96
72275 Z1 R	−1.53	1.15	1.15	0.33	0.33	0.23	0.10	4400	47	4452	88
NC-180 correction											
14163 Z89 R	−1.41	1.16	1.16	0.34	0.34	0.23	0.10	4353	47	4401	91
14163 Z9_L1	−1.23	1.04	1.05	0.27	0.27	0.17	0.10	4319	43	4361	86
14163 Z26_L1	0.91	1.51	1.51	0.57	0.57	0.33	0.24	4300	54	4269	115
14163 Z26_L2	−1.74	1.30	1.30	0.42	0.42	0.28	0.14	4327	51	4386	99
14321 Z3_L1	−1.87	1.22	1.22	0.37	0.37	0.27	0.10	4297	50	4360	98
14321 Z3_L2	−3.35	1.05	1.06	0.28	0.28	0.17	0.10	4355	43	4468	81
72275 Z1_L2	−0.53	1.08	1.08	0.29	0.29	0.19	0.11	4353	44	4371	88
72275 Z1_L1	−0.06	1.12	1.12	0.31	0.31	0.21	0.10	4338	46	4340	93
72275 Z1 R	−0.73	1.20	1.20	0.36	0.36	0.26	0.10	4367	49	4392	95

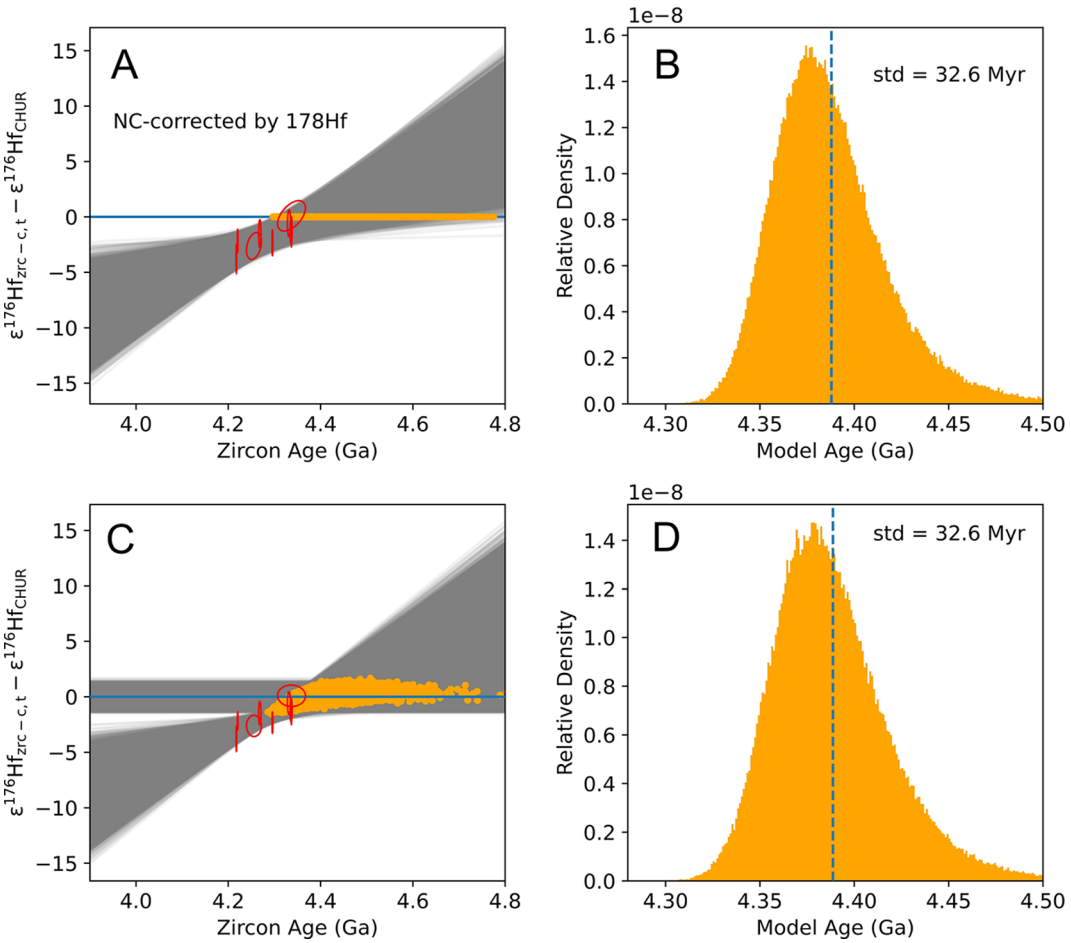

Figure 9. Example of how a zircon population model age can be calculated by regressing ε^{176}Hf against age (here neutron capture effects have been corrected for using ε^{178}Hf). Panel A shows an approach that includes uncertainties on CHUR parameters in the ε^{176}Hf value of each zircon, meaning that errors affecting different zircons will not be independent (eq 18). Panel C shows an approach that separates errors affecting zircons from CHUR (eqs 22 and 23). A Monte Carlo approach was used to calculate the reservoir model age and its uncertainty by calculating the intercept between a regression through the data and the CHUR reference. The histogram of the model ages from intercept points are plotted in panel B and D.

https://doi.org/10.1021/acsearthspacechem.3c00093
ACS Earth Space Chem. 2024, 8, 36−53

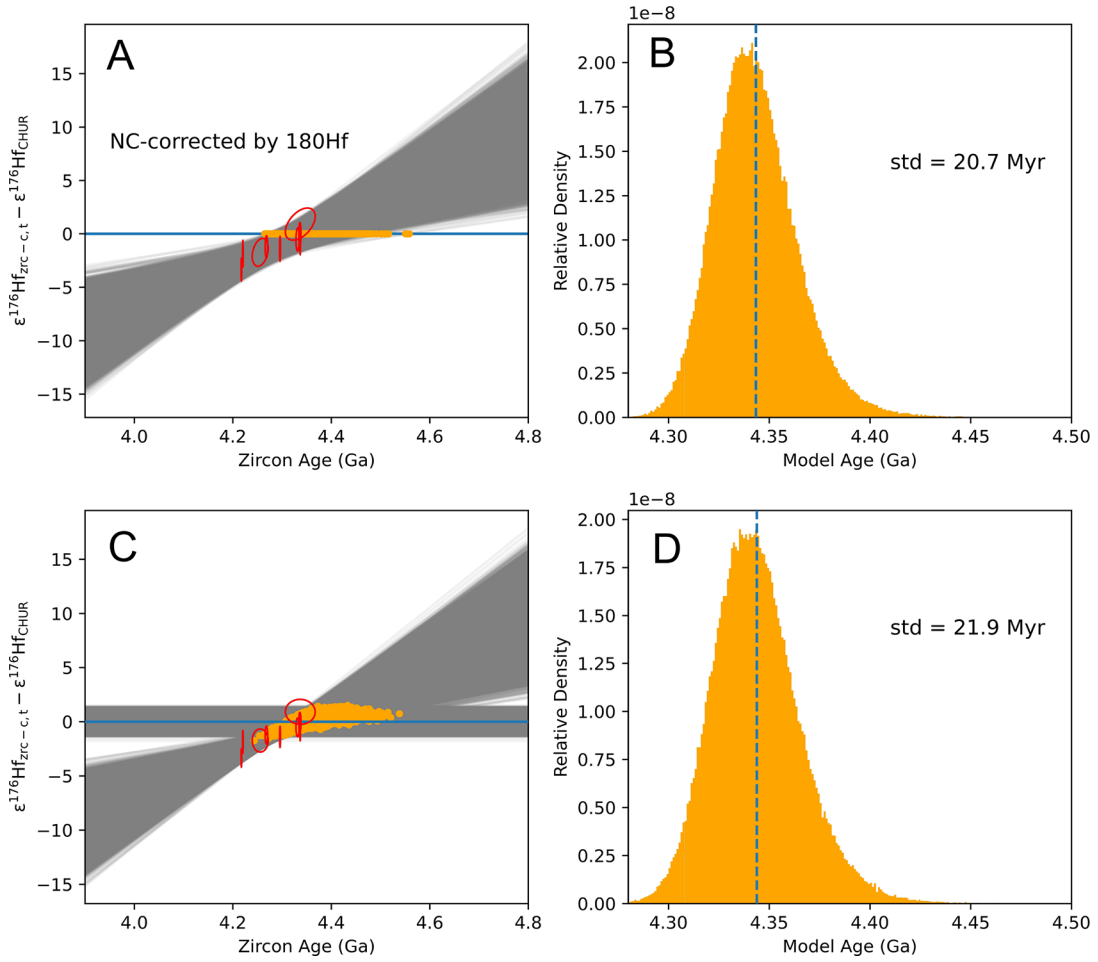

Figure 10. Example of how a zircon population model age can be calculated by regressing ε^{176}Hf against age (here neutron capture effects have been corrected for using ε^{180}Hf). Panel A shows an approach that includes uncertainties on CHUR parameters in the ε^{176}Hf value of each zircon, meaning that errors affecting different zircons will not be independent (eq 18). Panel C shows an approach that separates errors affecting zircons from CHUR (eqs 22 and 23). A Monte Carlo approach was used to calculate the reservoir model age and its uncertainty by calculating the intercept between a regression through the data and the CHUR reference. The histogram of the model ages from intercept points are plotted in panel B and D.

$$\left(\frac{^{176}\mathrm{Hf}}{^{177}\mathrm{Hf}}\right)_{\mathrm{zrc}-t,c} = \left(\frac{^{176}\mathrm{Hf}}{^{177}\mathrm{Hf}}\right)_{\mathrm{CHUR}-t} + \left[\left(\frac{^{176}\mathrm{Lu}}{^{177}\mathrm{Hf}}\right)_{\mathrm{R}-p} - \left(\frac{^{176}\mathrm{Lu}}{^{177}\mathrm{Hf}}\right)_{\mathrm{CHUR}-p}\right] (e^{\lambda_{^{176}\mathrm{Lu}}t_d} - e^{\lambda_{^{176}\mathrm{Lu}}t}) \quad (28)$$

After some rearrangements, the model age t_d can be expressed as,

$$t_d = \frac{1}{\lambda_{^{176}\mathrm{Lu}}}\ln\left[e^{\lambda_{^{176}\mathrm{Lu}}t} + \frac{(^{176}\mathrm{Hf}/^{177}\mathrm{Hf})_{\mathrm{CHUR}-t} - (^{176}\mathrm{Hf}/^{177}\mathrm{Hf})_{\mathrm{zrc}-t,c}}{(^{176}\mathrm{Lu}/^{177}\mathrm{Hf})_{\mathrm{CHUR}-p} - (^{176}\mathrm{Lu}/^{177}\mathrm{Hf})_{\mathrm{R}-p}}\right] \quad (29)$$

For KREEP, ^{176}Lu/^{177}Hf ratios of 0.0164,[10] 0.0154 ± 0.0034,[21] and 0.0153 ± 0.0033[22] were used by previous authors. Higher $(^{176}\mathrm{Lu}/^{177}\mathrm{Hf})_{\mathrm{R}-p}$ ratios result in higher model ages. A minimum model age can be calculated taking $(^{176}\mathrm{Lu}/^{177}\mathrm{Hf})_{\mathrm{R}-p} = 0$ in eq 29

$$t_d > \frac{1}{\lambda_{^{176}\mathrm{Lu}}}\ln\left[e^{\lambda_{^{176}\mathrm{Lu}}t} + \frac{(^{176}\mathrm{Hf}/^{177}\mathrm{Hf})_{\mathrm{CHUR}-t} - (^{176}\mathrm{Hf}/^{177}\mathrm{Hf})_{\mathrm{zrc}-t,c}}{(^{176}\mathrm{Lu}/^{177}\mathrm{Hf})_{\mathrm{CHUR-p}}}\right] \quad (30)$$

The uncertainties for individual best estimate or minimum model ages are also evaluated by using both MCS and analytical approaches. The analytical equations for propagating the uncertainties of model ages are provided in Supporting Information, and the two methods give the same errors for the model ages (Figure S1). An initial ^{176}Lu/^{177}Hf ratio of 0.0153 ± 0.0033 was used to estimate model ages for lunar zircons and the results are compiled in Table 5.

Another way to calculate a model age is to do a linear regression of $\varepsilon^{176}\mathrm{Hf}_{\mathrm{zrc}-t,c}$ versus the crystallization age (t) of all or a subset of zircons. This approach assumes that the population of zircons considered was all crystallized from an enriched reservoir that was isolated from CHUR at a set time. The intersection between the zircon regression line and CHUR gives the model age and the slope reflects the $(^{176}\mathrm{Lu}/^{177}\mathrm{Hf})_{\mathrm{R}-p}$ of the reservoir R. As an illustration, we used a Monte Carlo approach to calculate the intercept model age and $(^{176}\mathrm{Lu}/^{177}\mathrm{Hf})_{\mathrm{R}-p}$ ratio for the set of lunar zircons analyzed here. We generated a large random data set (200000) for both zircon ages and ε^{176}Hf following previous procedure for each zircon, and then sampled each zircon data point from the synthetic data set for a least-squares fitting (gray lines in Figures 9 and 10). The intersection with CHUR (orange points in Figures 9 and 10) was calculated by either using eqs 22 and 23 and treating CHUR as constant ($\varepsilon^{176}\mathrm{Hf}_{\mathrm{CHUR}-t/\overline{\mathrm{CHUR}-t}} = 0$) or using eq 18 and treating CHUR as a variable simulated using a Gaussian random number generator. In both cases, we calculated the slope and intersection of the CHUR line. The results of the two approaches are almost identical, yielding a

https://doi.org/10.1021/acsearthspacechem.3c00093
ACS Earth Space Chem. 2024, 8, 36−53

model age of 4388^{-48}_{+76} Ma (95% CI) and a $(^{176}Lu/^{177}Hf)_{R-p}$ ratio of 0.0079 ± 0.0098 when $\varepsilon^{178}Hf$ is used for correcting neutron capture effects. The model age and initial $(^{176}Lu/^{177}Hf)_{R-p}$ ratio are 4344^{-38}_{+48} Ma (95% CI) and 0.0082 ± 0.0098 when $\varepsilon^{180}Hf$ is used for correcting neutron capture effects. The reason we analyzed a small set of lunar zircons was to test our measurement protocol and data reduction pipeline on real samples. The zircon population analyzed here is too small to draw any conclusions about the history of LMO differentiation.

CONCLUSION

A procedure was developed for the purification and separation of Zr and Hf from zircons. The focus of this procedure was on the isotopic analysis of Hf in single zircon grains, but separation of Zr from Hf opens the door to isotopic analysis of Zr on the same samples. Hafnium isotopic analyses were done on MC-ICPMS, and we show that the precisions achieved are close to the theoretically attainable limit set by counting statistics and Johnson noise. We applied this technique to small zircon grains extracted from lunar samples returned by the Apollo missions. These zircon grains were chemically abraded and dated by U–Pb geochronology. The leachates from the chemical abrasion were passed through U–Pb chemistry before Hf purification. The zircon Hf isotopic analyses are corrected for *in situ* decay of ^{176}Lu, neutron capture effects associated with exposure to cosmic rays in space, and are reported relative to chondrites. Analysis of these zircons allows us to test all aspects of our measurement protocol and data reduction pipeline, which we will apply to more lunar samples to refine our understanding of the lunar impact and differentiation history.

ASSOCIATED CONTENT

Supporting Information

The Supporting Information is available free of charge at https://pubs.acs.org/doi/10.1021/acsearthspacechem.3c00093.

Calculation of zircon initial $\varepsilon^{176}Hf$ values using measured U–Pb ages, Lu/Hf ratios, neutron capture effects on $\varepsilon^{178}Hf$ and $\varepsilon^{180}Hf$, and error propagation and calculation of model ages of differentiation and error propagation (PDF)

Reduction of zircon Lu–Hf data (XLSX)

AUTHOR INFORMATION

Corresponding Author

Nicolas Dauphas − *Origins Laboratory, Department of the Geophysical Sciences and Enrico Fermi Institute, The University of Chicago, Chicago, Illinois 60637, United States;* orcid.org/0000-0002-1330-2038; Email: dauphas@uchicago.edu

Authors

Xi Chen − *Origins Laboratory, Department of the Geophysical Sciences and Enrico Fermi Institute, The University of Chicago, Chicago, Illinois 60637, United States*

Zhe J. Zhang − *Origins Laboratory, Department of the Geophysical Sciences and Enrico Fermi Institute, The University of Chicago, Chicago, Illinois 60637, United States;* orcid.org/0000-0001-8323-7967

Blair Schoene − *Department of Geosciences, Princeton University, Princeton, New Jersey 08544, United States*

Melanie Barboni − *CLAS-NS Departments, Arizona State University, Tempe, Arizona 85281, United States*

Ingo Leya − *Physics Institute, University of Bern, 3012 Bern, Switzerland*

Junjun Zhang − *Origins Laboratory, Department of the Geophysical Sciences and Enrico Fermi Institute, The University of Chicago, Chicago, Illinois 60637, United States*

Dawid Szymanowski − *Department of Geosciences, Princeton University, Princeton, New Jersey 08544, United States;* orcid.org/0000-0001-9524-5710

Kevin D. McKeegan − *Department of Earth, Planetary, and Space Sciences, University of California, Los Angeles, California 90095, United States*

Complete contact information is available at: https://pubs.acs.org/10.1021/acsearthspacechem.3c00093

Notes

The authors declare no competing financial interest.

ACKNOWLEDGMENTS

We thank two anonymous reviewers for their constructive comments that greatly improved the quality of the manuscript. This work was supported by NASA grant 80NSSC20K0821 (EW) to K.M., N.D., M.B., and B.S., as well as grants NNX17AE86G (LARS), 80NSSC17K0744 (HW), 000306-002 (HW), 80NSSC21K0380 (EW), NSF grant EAR-2001098 (CSEDI), and funding from DOE to N.D. and by the Swiss National Science Foundation (IL, 200020_196955).

REFERENCES

(1) Söderlund, U.; Patchett, P. J.; Vervoort, J. D.; Isachsen, C. E. The 176Lu decay constant determined by Lu–Hf and U–Pb isotope systematics of Precambrian mafic intrusions. *Earth and Planetary Science Letters* **2004**, *219* (3), 311–324.

(2) Barboni, M.; Boehnke, P.; Keller, B.; Kohl, I. E.; Schoene, B.; Young, E. D.; McKeegan, K. D. Early formation of the Moon 4.51 billion years ago. *Science Advances* **2017**, *3* (1), No. e1602365.

(3) Bauer, A.; Reimink, J.; Chacko, T.; Foley, B. J.; Shirey, S.; Pearson, D. Hafnium isotopes in zircons document the gradual onset of mobile-lid tectonics. *Geochemical Perspectives Letters* **2020**, *14*, 1–6.

(4) Blichert-Toft, J.; Albarède, F. Hafnium isotopes in Jack Hills zircons and the formation of the Hadean crust. *Earth and Planetary Science Letters* **2008**, *265* (3–4), 686–702.

(5) Bouvier, A.; Vervoort, J. D.; Patchett, P. J. The Lu–Hf and Sm-Nd isotopic composition of CHUR: constraints from unequilibrated chondrites and implications for the bulk composition of terrestrial planets. *Earth and Planetary Science Letters* **2008**, *273* (1–2), 48–57.

(6) Costa, M. M.; Jensen, N. K.; Bouvier, L. C.; Connelly, J. N.; Mikouchi, T.; Horstwood, M. S.; Suuronen, J.-P.; Moynier, F.; Deng, Z.; Agranier, A.; et al. The internal structure and geodynamics of Mars inferred from a 4.2-Gyr zircon record. *Proceedings of the National Academy of Sciences* **2020**, *117* (49), 30973–30979.

(7) Harrison, T.; Blichert-Toft, J.; Muller, W.; Albarede, F.; Holden, P.; Mojzsis, S. J. Heterogeneous Hadean hafnium: evidence of continental crust at 4.4 to 4.5 Ga. *Science* **2005**, *310* (5756), 1947–1950.

(8) Kemp, A.; Wilde, S.; Hawkesworth, C.; Coath, C.; Nemchin, A.; Pidgeon, R.; Vervoort, J.; DuFrane, S. Hadean crustal evolution revisited: new constraints from Pb-Hf isotope systematics of the Jack Hills zircons. *Earth and Planetary Science Letters* **2010**, *296* (1–2), 45–56.

(9) Stevenson, R. K.; Patchett, P. J. Implications for the evolution of continental crust from Hf isotope systematics of Archean detrital zircons. *Geochim. Cosmochim. Acta* **1990**, *54* (6), 1683–1697.

(10) Taylor, D. J.; McKeegan, K. D.; Harrison, T. M. Lu−Hf zircon evidence for rapid lunar differentiation. *Earth and Planetary Science Letters* **2009**, *279* (3−4), 157−164.
(11) D'Abzac, F.-X.; Davies, J. H. F. L.; Wotzlaw, J.-F.; Schaltegger, U. Hf isotope analysis of small zircon and baddeleyite grains by conventional Multi Collector-Inductively Coupled Plasma-Mass Spectrometry. *Chem. Geol.* **2016**, *433*, 12−23.
(12) Bauer, A. M.; Horstwood, M. S. A. Small-volume Lu−Hf and U−Pb isotope determination of complex zircons by solution and laser ablation MC-ICP-MS. *Chem. Geol.* **2018**, *476*, 85−99.
(13) Bast, R.; Scherer, E. E.; Sprung, P.; Fischer-Gödde, M.; Stracke, A.; Mezger, K. A rapid and efficient ion-exchange chromatography for Lu−Hf, Sm-Nd, and Rb-Sr geochronology and the routine isotope analysis of sub-ng amounts of Hf by MC-ICP-MS. *Journal of Analytical Atomic Spectrometry* **2015**, *30* (11), 2323−2333.
(14) Charlier, B.; Grove, T. L.; Namur, O.; Holtz, F. Crystallization of the lunar magma ocean and the primordial mantle-crust differentiation of the Moon. *Geochim. Cosmochim. Acta* **2018**, *234*, 50−69.
(15) Snyder, G. A.; Taylor, L. A.; Neal, C. R. A chemical model for generating the sources of mare basalts: Combined equilibrium and fractional crystallization of the lunar magmasphere. *Geochim. Cosmochim. Acta* **1992**, *56* (10), 3809−3823.
(16) Warren, P. H.; Wasson, J. T. The origin of KREEP. *Reviews of Geophysics* **1979**, *17* (1), 73−88.
(17) Warren, P. H. In KREEP: Major-element diversity, trace-element uniformity (almost). *Workshop on Moon in Transition: Apollo 14, KREEP, and Evolved Lunar Rocks*; Lunar and Planetary Institute, 1989; pp 149−153.
(18) Wielicki, M. M.; Harrison, T. M. Zircon formation in impact melts: Complications for deciphering planetary impact histories. *Large Meteorite Impacts and Planetary Evolution V: Geological Society of America Special Paper* **2015**, *518*, 127−134.
(19) Trail, D.; Barboni, M.; McKeegan, K. D. Evidence for diverse lunar melt compositions and mixing of the pre-3.9 Ga crust from zircon chemistry. *Geochim. Cosmochim. Acta* **2020**, *284*, 173−195.
(20) Borg, L. E.; Carlson, R. W. The Evolving Chronology of Moon Formation. *Annual Review of Earth and Planetary Sciences* **2023**, *51*, 25.
(21) Sprung, P.; Kleine, T.; Scherer, E. E. Isotopic evidence for chondritic Lu/Hf and Sm/Nd of the Moon. *Earth and Planetary Science Letters* **2013**, *380*, 77−87.
(22) Gaffney, A. M.; Borg, L. E. A young solidification age for the lunar magma ocean. *Geochim. Cosmochim. Acta* **2014**, *140*, 227−240.
(23) Greer, J.; Zhang, B.; Isheim, D.; Seidman, D. N.; Bouvier, A.; Heck, P. R. 4.46 Ga zircons anchor chronology of lunar magma ocean. *Geochemical Perspectives Letters* **2023**, *27*, 49−53.
(24) Bouvier, L. C.; Costa, M. M.; Connelly, J. N.; Jensen, N. K.; Wielandt, D.; Storey, M.; Nemchin, A. A.; Whitehouse, M. J.; Snape, J. F.; Bellucci, J. J.; et al. Evidence for extremely rapid magma ocean crystallization and crust formation on Mars. *Nature* **2018**, *558* (7711), 586−589.
(25) Iizuka, T.; Yamaguchi, T.; Hibiya, Y.; Amelin, Y. Meteorite zircon constraints on the bulk Lu−Hf isotope composition and early differentiation of the Earth. *Proceedings of the National Academy of Sciences* **2015**, *112* (17), 5331−5336.
(26) Blichert-Toft, J.; Chauvel, C.; Albarède, F. Separation of Hf and Lu for high-precision isotope analysis of rock samples by magnetic sector-multiple collector ICP-MS. *Contributions to Mineralogy and Petrology* **1997**, *127* (3), 248−260.
(27) Münker, C.; Weyer, S.; Scherer, E.; Mezger, K. Separation of high field strength elements (Nb, Ta, Zr, Hf) and Lu from rock samples for MC-ICPMS measurements. *Geochemistry, Geophysics, Geosystems* **2001**, *2* (12), 1064.
(28) Vervoort, J. D.; Kemp, A. I. S. Clarifying the zircon Hf isotope record of crust-mantle evolution. *Chem. Geol.* **2016**, *425*, 65−75.
(29) Peters, S. T. M.; Münker, C.; Wombacher, F.; Elfers, B.-M. Precise determination of low abundance isotopes (174Hf, 180W and 190Pt) in terrestrial materials and meteorites using multiple collector ICP-MS equipped with 1012Ω Faraday amplifiers. *Chem. Geol.* **2015**, *413*, 132−145.
(30) Feng, L.; Hu, W.; Jiao, Y.; Zhou, L.; Zhang, W.; Hu, Z.; Liu, Y. High-precision stable zirconium isotope ratio measurements by double spike thermal ionization mass spectrometry. *Journal of Analytical Atomic Spectrometry* **2020**, *35* (4), 736−745.
(31) He, S.; Li, Y.; Wu, L.-G.; Guo, D.-F.; Li, Z.-Y.; Li, X.-H. High precision zircon SIMS Zr isotope analysis. *Journal of Analytical Atomic Spectrometry* **2021**, *36* (10), 2063−2073.
(32) Ibañez-Mejia, M.; Tissot, F. L. Extreme Zr stable isotope fractionation during magmatic fractional crystallization. *Science Advances* **2019**, *5* (12), No. eaax8648.
(33) Inglis, E. C.; Creech, J. B.; Deng, Z.; Moynier, F. High-precision zirconium stable isotope measurements of geological reference materials as measured by double-spike MC-ICPMS. *Chem. Geol.* **2018**, *493*, 544−552.
(34) Inglis, E. C.; Moynier, F.; Creech, J.; Deng, Z.; Day, J. M.; Teng, F.-Z.; Bizzarro, M.; Jackson, M.; Savage, P. Isotopic fractionation of zirconium during magmatic differentiation and the stable isotope composition of the silicate Earth. *Geochim. Cosmochim. Acta* **2019**, *250*, 311−323.
(35) Méheut, M.; Ibañez-Mejia, M.; Tissot, F. L. Drivers of zirconium isotope fractionation in Zr-bearing phases and melts: the roles of vibrational, nuclear field shift and diffusive effects. *Geochimica et cosmochimica acta* **2021**, *292*, 217−234.
(36) Tian, S.; Moynier, F.; Inglis, E.; Creech, J.; Bizzarro, M.; Siebert, J.; Day, J.; Puchtel, I. Zirconium isotopic composition of the mantle through time. *Geochemical Perspectives Letters* **2020**, *15*, 40−43.
(37) Tompkins, H. G.; Zieman, L. J.; Ibanez-Mejia, M.; Tissot, F. L. Zirconium stable isotope analysis of zircon by MC-ICP-MS: methods and application to evaluating intra-crystalline zonation in a zircon megacryst. *Journal of Analytical Atomic Spectrometry* **2020**, *35* (6), 1167−1186.
(38) Yuan, Y.; Guo, J.-L.; Zong, K.; Feng, L.; Wang, Z.; Moynier, F.; Zhang, W.; Hu, Z.; Xu, H. Stable zirconium isotopic fractionation during alkaline magma differentiation: Implications for the differentiation of continental crust. *Geochim. Cosmochim. Acta* **2022**, *326*, 41−55.
(39) Zhang, W.; Wang, Z.; Moynier, F.; Inglis, E.; Tian, S.; Li, M.; Liu, Y.; Hu, Z. Determination of Zr isotopic ratios in zircons using laser-ablation multiple-collector inductively coupled-plasma mass-spectrometry. *Journal of Analytical Atomic Spectrometry* **2019**, *34* (9), 1800−1809.
(40) Akram, W.; Schönbächler, M.; Bisterzo, S.; Gallino, R. Zirconium isotope evidence for the heterogeneous distribution of s-process materials in the solar system. *Geochim. Cosmochim. Acta* **2015**, *165*, 484−500.
(41) Akram, W.; Schönbächler, M.; Sprung, P.; Vogel, N. Zirconium—Hafnium isotope evidence from meteorites for the decoupled synthesis of light and heavy neutron-rich nuclei. *The Astrophysical Journal* **2013**, *777* (2), 169.
(42) Elfers, B.-M.; Sprung, P.; Messling, N.; Münker, C. The combined Zr and Hf isotope inventory of bulk rock and sequentially leached chondrite samples. *Geochim. Cosmochim. Acta* **2020**, *270*, 475−491.
(43) Render, J.; Brennecka, G. A.; Burkhardt, C.; Kleine, T. Solar System evolution and terrestrial planet accretion determined by Zr isotopic signatures of meteorites. *Earth and Planetary Science Letters* **2022**, *595*, 117748.
(44) Sanloup, C.; Blichert-Toft, J.; Télouk, P.; Gillet, P.; Albarède, F. Zr isotope anomalies in chondrites and the presence of 92Nb in the early solar system. *Earth and Planetary Science Letters* **2000**, *184* (1), 75−81.
(45) Schönbächler, M.; Lee, D.-C.; Rehkämper, M.; Halliday, A. N.; Fehr, M. A.; Hattendorf, B.; Günther, D. Zirconium isotope evidence for incomplete admixing of r-process components in the solar nebula. *Earth and Planetary Science Letters* **2003**, *216* (4), 467−481.
(46) Harper, C. L., Jr. Evidence for 92gNb in the early solar system and evaluation of a new p-process cosmochronometer from 92gNb/92Mo. *The Astrophysical Journal* **1996**, *466*, 437.

(47) Hibiya, Y.; Iizuka, T.; Enomoto, H.; Hayakawa, T. Evidence for Enrichment of Niobium-92 in the Outer Protosolar Disk. *The Astrophysical Journal Letters* **2023**, *942* (1), L15.
(48) Iizuka, T.; Lai, Y.-J.; Akram, W.; Amelin, Y.; Schönbächler, M. The initial abundance and distribution of 92Nb in the Solar System. *Earth and Planetary Science Letters* **2016**, *439*, 172−181.
(49) Schönbächler, M.; Rehkämper, M.; Halliday, A. N.; Lee, D.-C.; Bourot-Denise, M.; Zanda, B.; Hattendorf, B.; Günther, D. Niobium-Zirconium Chronometry and Early Solar System Development. *Science* **2002**, *295* (5560), 1705−1708.
(50) Zhang, J., *Titanium Isotope Cosmochemistry*; The University of Chicago, 2012.
(51) Horwitz, E.; McAlister, D.; Bond, A.; Barrans, R., Jr Novel extraction of chromatographic resins based on tetraalkyldiglycolamides: characterization and potential applications. *Solvent extraction and ion exchange* **2005**, *23* (3), 319−344.
(52) Pourmand, A.; Dauphas, N. Distribution coefficients of 60 elements on TODGA resin: application to Ca, Lu, Hf, U and Th isotope geochemistry. *Talanta* **2010**, *81* (3), 741−753.
(53) Zhang, J.; Dauphas, N.; Davis, A. M.; Pourmand, A. A new method for MC-ICPMS measurement of titanium isotopic composition: Identification of correlated isotope anomalies in meteorites. *Journal of Analytical Atomic Spectrometry* **2011**, *26* (11), 2197−2205.
(54) Fisher, C. M.; Hanchar, J. M.; Samson, S. D.; Dhuime, B.; Blichert-Toft, J.; Vervoort, J. D.; Lam, R. Synthetic zircon doped with hafnium and rare earth elements: A reference material for in situ hafnium isotope analysis. *Chem. Geol.* **2011**, *286* (1), 32−47.
(55) Chen, X.; Wang, W.; Zhang, Z.; Nie, N. X.; Dauphas, N. Evidence from Ab Initio and Transport Modeling for Diffusion-Driven Zirconium Isotopic Fractionation in Igneous Rocks. *ACS Earth Space Chem.* **2020**, *4* (9), 1572−1595.
(56) Chu, N.-C.; Taylor, R. N.; Chavagnac, V.; Nesbitt, R. W.; Boella, R. M.; Milton, J. A.; German, C. R.; Bayon, G.; Burton, K. Hf isotope ratio analysis using multi-collector inductively coupled plasma mass spectrometry: an evaluation of isobaric interference corrections. *Journal of Analytical Atomic Spectrometry* **2002**, *17* (12), 1567−1574.
(57) Jonathan Patchett, P.; Kouvo, O.; Hedge, C. E.; Tatsumoto, M. Evolution of continental crust and mantle heterogeneity: Evidence from Hf isotopes. *Contributions to Mineralogy and Petrology* **1982**, *78* (3), 279−297.
(58) Maréchal, C. N.; Télouk, P.; Albarède, F. Precise analysis of copper and zinc isotopic compositions by plasma-source mass spectrometry. *Chem. Geol.* **1999**, *156* (1), 251−273.
(59) Blichert-Toft, J.; Albarède, F. The Lu−Hf isotope geochemistry of chondrites and the evolution of the mantle-crust system. *Earth and Planetary Science Letters* **1997**, *148* (1), 243−258.
(60) Dauphas, N.; Chen, J. H.; Zhang, J.; Papanastassiou, D. A.; Davis, A. M.; Travaglio, C. Calcium-48 isotopic anomalies in bulk chondrites and achondrites: Evidence for a uniform isotopic reservoir in the inner protoplanetary disk. *Earth and Planetary Science Letters* **2014**, *407*, 96−108.
(61) Woodhead, J. D.; Hergt, J. M. A preliminary appraisal of seven natural zircon reference materials for in situ Hf isotope determination. *Geostandards and Geoanalytical Research* **2005**, *29* (2), 183−195.
(62) Dauphas, N.; Marty, B.; Reisberg, L. Molybdenum Evidence for Inherited Planetary Scale Isotope Heterogeneity of the Protosolar Nebula. *The Astrophysical Journal* **2002**, *565* (1), 640.
(63) Dauphas, N.; Schauble, E. A. Mass fractionation laws, mass-independent effects, and isotopic anomalies. *Annual Review of Earth and Planetary Sciences* **2016**, *44*, 709−783.
(64) Elfers, B.-M.; Sprung, P.; Pfeifer, M.; Wombacher, F.; Peters, S. T. M.; Münker, C. Variable distribution of s-process Hf and W isotope carriers in chondritic meteorites - Evidence from 174Hf and 180W. *Geochim. Cosmochim. Acta* **2018**, *239*, 346−362.
(65) Qin, L.; Carlson, R. W.; Alexander, C. M. O. D. Correlated nucleosynthetic isotopic variability in Cr, Sr, Ba, Sm, Nd and Hf in Murchison and QUE 97008. *Geochim. Cosmochim. Acta* **2011**, *75* (24), 7806−7828.
(66) Sprung, P.; Scherer, E. E.; Upadhyay, D.; Leya, I.; Mezger, K. Non-nucleosynthetic heterogeneity in non-radiogenic stable Hf isotopes: Implications for early solar system chronology. *Earth and Planetary Science Letters* **2010**, *295* (1), 1−11.
(67) Dauphas, N.; Davis, A. M.; Marty, B.; Reisberg, L. The cosmic molybdenum-ruthenium isotope correlation. *Earth and Planetary Science Letters* **2004**, *226* (3), 465−475.
(68) Bisterzo, S.; Gallino, R.; Straniero, O.; Cristallo, S.; Käppeler, F. The s-process in low-metallicity stars - II. Interpretation of high-resolution spectroscopic observations with asymptotic giant branch models. *Mon. Not. R. Astron. Soc.* **2011**, *418* (1), 284−319.
(69) Mattinson, J. M. Zircon U−Pb chemical abrasion ("CA-TIMS") method: combined annealing and multi-step partial dissolution analysis for improved precision and accuracy of zircon ages. *Chem. Geol.* **2005**, *220* (1−2), 47−66.
(70) Condon, D. J.; Schoene, B.; McLean, N. M.; Bowring, S. A.; Parrish, R. R. Metrology and traceability of U−Pb isotope dilution geochronology (EARTHTIME Tracer Calibration Part I). *Geochim. Cosmochim. Acta* **2015**, *164*, 464−480.
(71) McLean, N. M.; Condon, D. J.; Schoene, B.; Bowring, S. A. Evaluating uncertainties in the calibration of isotopic reference materials and multi-element isotopic tracers (EARTHTIME Tracer Calibration Part II). *Geochim. Cosmochim. Acta* **2015**, *164*, 481−501.
(72) Krogh, T. E. A low-contamination method for hydrothermal decomposition of zircon and extraction of U and Pb for isotopic age determinations. *Geochim. Cosmochim. Acta* **1973**, *37* (3), 485−494.
(73) Gerstenberger, H.; Haase, G. A highly effective emitter substance for mass spectrometric Pb isotope ratio determinations. *Chemical geology* **1997**, *136* (3−4), 309−312.
(74) Koning, A.; Forrest, R.; Kellett, M.; Mills, R.; Henriksson, H.; Rugama, Y.; Bersillon, O.; Bouland, O.; Courcelle, A.; Duijvestijn, M. *The Jeff-3.1 Nuclear Data Library—Jeff Report 21*; Organisation for Economic Co-operation and Development, 2006.
(75) Plompen, A. J.; Cabellos, O.; De Saint Jean, C.; Fleming, M.; Algora, A.; Angelone, M.; Archier, P.; Bauge, E.; Bersillon, O.; Blokhin, A.; et al. The joint evaluated fission and fusion nuclear data library, JEFF-3.3. *The European Physical Journal A* **2020**, *56*, 181.
(76) Brown, D. A.; Chadwick, M.; Capote, R.; Kahler, A.; Trkov, A.; Herman, M.; Sonzogni, A.; Danon, Y.; Carlson, A.; Dunn, M.; et al. ENDF/B-VIII. 0: the 8th major release of the nuclear reaction data library with CIELO-project cross sections, new standards and thermal scattering data. *Nuclear Data Sheets* **2018**, *148*, 1−142.
(77) Schoene, B.; Eddy, M. P.; Samperton, K. M.; Keller, C. B.; Keller, G.; Adatte, T.; Khadri, S. F. U−Pb constraints on pulsed eruption of the Deccan Traps across the end-Cretaceous mass extinction. *Science* **2019**, *363* (6429), 862−866.
(78) O'Connor, L.; Szymanowski, D.; Eddy, M. P.; Samperton, K. M.; Schoene, B. A red bole zircon record of cryptic silicic volcanism in the Deccan Traps, India. *Geology* **2022**, *50* (4), 460−464.
(79) Sláma, J.; Košler, J.; Condon, D. J.; Crowley, J. L.; Gerdes, A.; Hanchar, J. M.; Horstwood, M. S. A.; Morris, G. A.; Nasdala, L.; Norberg, N.; Schaltegger, U.; Schoene, B.; Tubrett, M. N.; Whitehouse, M. J. Plešovice zircon — A new natural reference material for U−Pb and Hf isotopic microanalysis. *Chem. Geol.* **2008**, *249* (1), 1−35.
(80) Connelly, J. N.; Bizzarro, M.; Krot, A. N.; Nordlund, A.; Wielandt, D.; Ivanova, M. A. The Absolute Chronology and Thermal Processing of Solids in the Solar Protoplanetary Disk. *Science* **2012**, *338* (6107), 651−655.
(81) Dauphas, N.; Hopp, T.; Craig, G.; Zhang, Z. J.; Valdes, M. C.; Heck, P. R.; Charlier, B. L.; Bell, E. A.; Harrison, T. M.; Davis, A. M.; et al. In situ 87 Rb-87 Sr analyses of terrestrial and extraterrestrial samples by LA-MC-ICP-MS/MS with double Wien filter and collision cell technologies. *Journal of Analytical Atomic Spectrometry* **2022**, *37* (11), 2420−2441.

https://doi.org/10.1021/acsearthspacechem.3c00093
ACS Earth Space Chem. 2024, 8, 36−53